Triclosan depletes the membrane potential in *Pseudomonas aeruginosa* biofilms inhibiting aminoglycoside induced adaptive resistance

Michael M. Maiden and Christopher M. Waters*

[1]Departments of Microbiology and Molecular Genetics and The BEACON Center for The Study of Evolution in Action, Michigan State University, East Lansing, Michigan, United States of America

*Corresponding Author

E-mail: watersc3@msu.edu (CW)

Abstract

Biofilm-based infections are difficult to treat due to their inherent resistance to antibiotic treatment. Discovering new approaches to enhance antibiotic efficacy in biofilms would be highly significant in treating many chronic infections. Exposure to aminoglycosides induces adaptive resistance in *Pseudomonas aeruginosa* biofilms. Adaptive resistance is primarily the result of active antibiotic export by RND-type efflux pumps, which use the proton motive force as an energy source. We show that the protonophore uncoupler triclosan depletes the membrane potential of biofilm growing *P. aeruginosa*, leading to decreased activity of RND-type efflux pumps. This disruption results in increased intracellular accumulation of tobramycin and enhanced antimicrobial activity *in vitro*. In addition, we show that triclosan enhances tobramycin effectiveness *in vivo* using a mouse wound model. Combining triclosan with tobramycin is a new anti-biofilm strategy that targets bacterial energetics, increasing the susceptibility of *P. aeruginosa* biofilms to aminoglycosides.

Author summary

Adaptive resistance is a phenotypic response that allows *P. aeruginosa* to transiently survive aminoglycosides such as tobramycin. To date, few compounds have been identified that target adaptive resistance. Here, we show the protonophore uncoupler triclosan disrupts the membrane potential of *P. aeruginosa*. The depletion of the membrane potential reduces efflux pump activity, which is essential for adaptive resistance, leading to increased tobramycin accumulation and a shorter onset of action. Our results demonstrate that in addition to its canonical mechanism inhibiting membrane biosynthesis, triclosan can exert antibacterial properties by functioning as a protonophore that targets *P. aeruginosa* energetics.

Introduction

Pseudomonas aeruginosa is a Gram-negative opportunistic pathogen that can form highly recalcitrant biofilms in immunocompromised hosts such as those suffering from cystic fibrosis (CF) and diabetes (1-4). Biofilms are a community of cells enmeshed in a self-made matrix that is highly tolerant to antibiotic treatment (1-4). In addition to biofilm growth, *P. aeruginosa* possesses many antibiotic resistance mechanisms including low outer membrane (OM) permeability, which is estimated to be $1/100^{th}$ that of *Escherichia coli* (5), the expression of proton motive force (PMF) dependent resistance-nodulation-cell division (RND) family of multidrug efflux pumps, and a chromosomal encoded AmpC β-lactamase, making it naturally resistant to β-lactams (4).

P. aeruginosa also exhibits a unique form of adaptive resistance in response to aminoglycosides, cationic antimicrobial peptides, and polymyxins (6, 7). Adaptive resistance is mainly mediated by the induction of RND-type efflux pumps and by alterations to the OM within 2-hrs of exposure to subinhibitory concentrations of aminoglycosides (8-11). Aminoglycosides cause the mistranslation of the PA5471 leader peptide PA5471.1, a peptide which inhibits the MexZ repressor, thereby triggering the induction of the RND-type efflux pump MexXY (12). This phenomenon has been observed *in vitro,* in animal models, and in CF patients (13-17).

Aminoglycoside uptake occurs in three steps (18-20). In the first step, termed "self-promoted uptake," positively charged aminoglycosides bind negatively charged components of the OM, triggering permeabilization and diffusion (18-20). In the second step, energy dependent phase-I (EDP-I), aminoglycosides slowly cross the inner membrane (IM) dependent upon the membrane potential ($\Delta\psi$) (18-20). In the third step, EDP-II, aminoglycosides bind to the A-site

of the 30S subunit of membrane-associated ribosomes and cause the synthesis of misfolded proteins that insert into the IM triggering permeabilization of the cytosolic barrier (18-20). This leads to an irreversible entry of aminoglycosides into the cell, thereby inhibiting translation.

Despite the well-documented phenomenon of adaptive resistance, aminoglycosides continue to be the standard of care for pseudomonal infections (21). In fact, pulmonary infections in CF patients are treated with extended doses of the aminoglycoside tobramycin (300-mg nebulized twice-a-day for 28-days), reaching mean sputum concentrations of ~737 µg/g per dose (21, 22). As antibacterial resistance continues to be an emerging public health crisis, there is a crucial need for new therapeutic approaches that decrease resistance (23). One approach is to target bacterial energetics (24). The feasibility of this approach was recently demonstrated by the discovery of the protonophore uncoupler bedaquiline, which is the first new Food and Drug Administration (FDA) approved *Mycobacterium tuberculosis* (*Mtb*) drug in 40-years (25-27).

We previously performed a high throughput screen (HTS) to identify compounds that enhanced tobramycin against *P. aeruginosa* biofilms and unexpectedly discovered that the combination of triclosan and tobramycin (or other aminoglycosides) was 100-times more effective than either triclosan, tobramycin, or other aminoglycosides alone at killing established *P. aeruginosa* biofilms (28). Triclosan is a fatty acid synthesis inhibitor, targeting the enoyl-acyl carrier reductase FabI (29). However, it is well-known that *P. aeruginosa* is inherently resistant to triclosan due to the expression of both the RND-type efflux pump TriABC and a triclosan resistant enoyl-acyl carrier reductase FabV, and our previous results suggested that triclosan does not enhance tobramycin activity by targeting FabI (28, 30, 31). Therefore, the mechanism of action of triclosan enhancement of aminoglycoside activity remained unknown.

The PMF is the sum of the membrane potential due to charge separation ($\Delta\psi$, positive$_{outside}$/negative$_{inside}$) and the proton gradient (ΔpH, acidic$_{outside}$/alkaline$_{inside}$) across the inner membrane (32, 33). Recently, it has been shown that in addition to fatty acid synthesis inhibition, triclosan possesses protonophore activity that can disrupt the $\Delta\psi$ of mitochondria isolated from rats, artificial bilayer lipid membranes, and the Gram-positive bacterium *Bacillus subtilis* (34-38). This led us to hypothesize that triclosan enhances aminoglycoside activity by targeting the $\Delta\psi$ in *P. aeruginosa* (28). In fact, from the same HTS in which triclosan was identified, we discovered that the protonophore uncoupler oxyclozanide acted synergistically with tobramycin to kill *P. aeruginosa* biofilms (39).

Here we demonstrate that triclosan increases *P. aeruginosa* susceptibility to tobramycin by disrupting adaptive resistance. This occurs because triclosan decreases the $\Delta\psi$, leading to a reduction in the activity of RND-type efflux pumps, which increases tobramycin accumulation within cells. Finally, we demonstrate that triclosan in combination with tobramycin embedded in a hydrogel is effective *in vivo* using a murine wound model. As numerous toxicity studies have demonstrated that triclosan is safe when used appropriately (40-42), this combination has the clinical potential to improve the treatment of biofilm-based infections by targeting bacterial energetics.

Results

The disruption of fatty acid synthesis does not increase *P. aeruginosa* susceptibility to tobramycin.

To determine if the inhibition of fatty acid biosynthesis and membrane biogenesis by triclosan is responsible for increasing *P. aeruginosa* susceptibility to tobramycin, we tested if the specific fatty acid synthesis inhibitor AFN-1252 synergized with tobramycin to kill *P. aeruginosa* biofilms. AFN-1252 forms a binary complex with the active site of FabI, which is an enoyl-acyl reductase responsible for the final elongation step in fatty acid synthesis and is inhibited by triclosan (43).

AFN-1252 alone and in combination with tobramycin was not effective at killing biofilms (Fig. S1). At the maximal concentrations of tobramycin and AFN-1252 used we observed slightly more than 2-fold killing; however, this difference was not statistically significant and far weaker than the ~100-fold killing observed when triclosan is combined with tobramycin (28). These findings are in agreement with our previous genetic experiments using a FabI mutant of *P. aeruginosa* that showed identical resistance to tobramycin treatment as the parental strain (28). Together, both our genetic and molecular experiments suggest that the inhibition of FabI by triclosan does not account for increased *P. aeruginosa* susceptibility to tobramycin.

Triclosan combined with tobramycin causes synergistic permeabilization of cells within biofilms.

Aminoglycosides corrupt protein synthesis by binding to the A-site of the 30S subunit of membrane bound ribosomes causing mistranslation of membrane proteins and inner membrane

134 permeabilization (18-20). We initially hypothesized that triclosan enhanced tobramycin killing
135 by permeabilizing cells in biofilms. To test this hypothesis, we stained cells with the cell-
136 impermeant TO-PRO™-3 iodide dye, which selectively emits a fluorescent signal in
137 permeabilized cells.

138 Treatment for 2-hrs with triclosan or tobramycin alone resulted in ~15% and ~11% of the
139 cells within biofilms to become permeabilized, respectively (Fig. 1). Neither of these increases
140 were statistically significantly compared to untreated controls. Alternatively, the combination of
141 triclosan and tobramycin permeabilized ~50% of cells after only 2-hrs of treatment. This result
142 suggests that neither triclosan nor tobramycin treatment alone is sufficient to permeabilize *P.*
143 *aeruginosa* cells growing in biofilms.

144

145 **Mutations in *fusA1* are resistant to the combination.**

146 To further elucidate the mechanism of action of this combination, we selected for
147 resistance mutants and then performed whole genome sequencing to identify causative
148 mutations, using a modified method developed by Lindsey et al. (44). 27 *P. aeruginosa* biofilms
149 serially passaged in parallel were exposed to sudden, moderate and gradual treatment regimens
150 consisting of ever-increasing concentrations of tobramycin and triclosan (Table S1). No resistant
151 mutations were isolated from populations exposed to sudden or moderate treatment regimens.
152 After 30 passages, two resistant populations from the gradual treatment regimen were isolated
153 (Table 1), and 96-colonies were isolated from each mutant pool that were found to be resistant to
154 the combination.

155 To determine the mutation(s) responsible for the resistance to the combination we
156 performed whole genome sequencing on two mutants from the F1 and four mutants from the B2

157 mutant populations (Table 1). These 6 mutants all showed complete resistance to tobramycin and
158 partial resistance to the combination compared to the ancestral strain (Fig. 2). The low level of
159 killing generated by the combination may be attributed to triclosan as all six of these mutants
160 exhibited increased sensitivity to triclosan treatment alone versus the ancestral strain. This
161 phenomenon, termed "collateral sensitivity," is the process by which resistance to one
162 antimicrobial simultaneously results in increased sensitivity to unrelated antimicrobials (45).
163 One common feature of all six mutants was a single nucleotide polymorphism (SNP) in
164 the *fusA1* gene encoding for EF-G1A, a protein responsible for ribosomal translocation and
165 recycling (46). Two unique mutations, a SNP at residues L40Q or T64A were identified. These
166 mutations are near or within the switch I domain, respectively, which is required for hydrolysis
167 of guanosine triphosphate and the "power-stroke" of EF-G1A. Because all mutants having a
168 L40Q SNP came from mutant pool F1 and all mutants having a T64A SNP came from mutant
169 pool B2, we hypothesize that these SNPs occurred early on during selection, allowing for clonal
170 expansion. However, no two isolates have the exact same set of SNPs, indicating the sequenced
171 strains are not siblings and each isolate is a distinct mutant as detailed in the discussion
172 (supplemental spreadsheet). Importantly, mutations in *fusA1* that have been found in clinical
173 isolates, including L40Q, confer resistance to tobramycin through an unknown mechanism (47).
174 Together, these results suggest that tobramycin is the component of the combination that is
175 primarily responsible for killing.
176

177 **Initial tobramycin treatment is required for the combination to be effective.**

178 The corruption of translation is thought to be the first step in aminoglycoside induced
179 adaptive resistance (12). This led us to hypothesize that tobramycin must first corrupt translation

thereby triggering adaptive resistance and the induction of RND-type efflux pumps for the combination to be synergistic (8-10, 12). To test if tobramycin induction of adaptive resistance was important for synergy, we first treated *P. aeruginosa* biofilms with tobramycin alone for 3-hrs and then washed the biofilms three time in Dulbecco's Phosphate Buffer Solution (DPBS) for 3-mins each followed by subsequent treatment with triclosan alone for 3-hrs. We performed a similar experiment first treating with triclosan followed by tobramycin treatment.

Sequential treatment with tobramycin followed by triclosan addition caused synergy, resulting in ~2-$\log_{10}$ reduction in cells within biofilms compared to untreated controls (Fig. S2). Intriguingly, despite no longer having tobramycin in the media, the cells within the biofilms were killed when treated with triclosan. We speculate that enough tobramycin remains after washing due to association of aminoglycosides with the extracellular polymeric substances (EPSs) making up the biofilm matrix and cell itself, which has been demonstrated to be resistant to removal by washing (19, 48). Alternatively, initial treatment with triclosan followed by treatment with tobramycin did not cause synergy or result in significant biofilm killing. These data suggest that a phenotypic switch induced by aminoglycoside exposure is important for synergistic activity.

In support of these experiments, we previously showed that tobramycin induces classic adaptive resistance, rendering *P. aeruginosa* refractory to killing by tobramycin until 6-hours, with the greatest resistance observed at 2-hrs (28). Furthermore, we found that only antibiotics that corrupt translation (aminoglycosides and tetracycline) act synergistically or are enhanced when combined with triclosan (28). Our past and current results lead us to hypothesize that tobramycin triggers adaptive resistance, which is then disrupted by triclosan.

Triclosan reduces RND-type efflux pump activity.

Because RND-type efflux pumps are a major component of aminoglycoside induced adaptive resistance (8-10, 12), we measured their activity in biofilms after treatment with tobramycin alone or in combination with triclosan by measuring cellular accumulation of ethidium bromide. Ethidium bromide is a substrate of RND-type efflux pumps, and its accumulation within cells can be used as a proxy for their activity (49). In this assay, the protonophore carbonyl cyanide 3-chlorophenylhydrazone (CCCP), which is known to reduce efflux pump activity, was used as a positive control (49). CCCP treatment led to increased ethidium bromide accumulation in *P. aeruginosa* biofilms as expected (Fig. 3). Similarly, triclosan reduced efflux pump activity as indicated by increased ethidium bromide accumulation, but tobramycin treatment alone had no effect. The combination of triclosan and tobramycin was similar to triclosan alone. These data suggest that triclosan reduces the activity of RND-type efflux pumps.

Triclosan increased intercellular accumulation of tobramycin.

Triclosan inhibition of RND-type efflux pumps should increase the accumulation of tobramycin within cells. To test this, we conjugated tobramycin with the fluorescent Texas Red dye (TbTR) as previously described (50), and measured its accumulation within cells growing as biofilms. Conversely, we also measured TbTR extrusion from cells into treatment-free recovery media.

For accumulation assays, biofilms were treated with TbTR with and without triclosan for 30-mins. Based on our previously published time-killing studies, this time point is before the

combination causes cell death (28). Prior to reading fluorescence, biofilms were washed, mechanically disrupted with a wooden stick, and cells were lysed to release TbTR. Triclosan in combination with TbTR resulted in a statistically significant increase in TbTR accumulation whereas CCCP did not significantly increase TbTR accumulation (Fig. 4A). This is in agreement with CCCPs reduced potency compared to triclosan at disrupting the membrane potentials of bacteria due to differences in lipophilicity and reduced activity against RND-type efflux pumps in *P. aeruginosa* biofilms (36).

To confirm that co-treatment with triclosan increased tobramycin accumulation within cells, biofilms were treated with TbTR with and without triclosan for 30-mins. Then biofilms were washed three-times in DPBS, recovered in treatment-free media for 30-mins and the supernatant was measured. Triclosan in combination with TbTR resulted in greater overall extrusion into treatment-free media, indicating more TbTR had accumulated in cells prior to recovery (Fig. 4B). These results support the conclusion that triclosan reduces the activity of RND-type efflux pumps, leading to increased accumulation of TbTR within cells.

Triclosan inhibits tobramycin induced Δψ.

Triclosan has a hydroxyl group with a dissociable proton that can disrupt the Δψ in eukaryotic cells, mitochondria, and bacteria (34-38). Because adaptive resistance is primarily the result of PMF driven RND-type efflux pumps (8-10, 12), we speculated that the depletion of the Δψ could lead to their inhibition and the abolishment of adaptive resistance. In these experiments, we measured changes in the Δψ rather than the ΔpH because at neutral pH the PMF in bacteria is primarily composed of the Δψ due to homeostatic buffering (51, 52), and RND-type efflux pump activity is primarily driven by the Δψ which is generated more rapidly than

248 ΔpH (53, 54). To measure changes in the Δψ of *P. aeruginosa* growing as biofilms, cells were
249 stained with the fluorescent Δψ indicator DiOC2(3) dye and analyzed by flow cytometry. Cells
250 were also co-stained with the membrane impermeant TO-PRO™-3 iodide dye to exclude
251 permeabilized cells from analysis of Δψ.

252 Triclosan treatment for 2-hrs reduced the population of cells maintaining a Δψ 4-fold,
253 from ~20% to ~5% (Fig. 5). Tobramycin treatment resulted in an increase in the population of
254 cells with a Δψ almost 2-fold, from ~20% to ~37%. This increase is indicative of adaptive
255 resistance (8-10, 12). Triclosan in addition to tobramycin reduced the population of cells
256 maintaining a Δψ almost 4-fold from tobramycin treatment alone to levels comparable to
257 untreated biofilms. These data suggest that triclosan depletes the Δψ at an essential time in
258 aminoglycoside induced adaptive resistance when a surge in the Δψ is protective against
259 tobramycin by increasing RND-type efflux pump activity.

260

261 **Methyl-triclosan does not disrupt the membrane potential or synergize with tobramycin.**

262 To confirm that protonophore activity by triclosan is responsible for tobramycin
263 enhancement, we treated cells with the chemical derivative methyl-triclosan, which lacks the
264 hydroxyl moiety necessary for gaining and losing a proton and therefore cannot act as a
265 protonophore (35). In addition, without this hydroxyl group, methyl-triclosan cannot inhibit fatty
266 acid synthesis by forming a complex with the co-factors NADH/NAD+ (35).

267 We first performed biofilm susceptibility testing using methyl-triclosan alone and in
268 combination with tobramycin. Neither methyl-triclosan nor the combination were effective
269 against biofilms after 6-hrs of treatment over a range of concentrations (Fig. S3). Furthermore,
270 methyl-triclosan had no effect on the population of cells maintaining a Δψ compared to untreated

biofilms and did not reduce the tobramycin induced surge in $\Delta\psi$ after 2-hrs of treatment (Fig. S4A). In addition, methyl-triclosan did not cause permeabilization of cells alone or in combination with tobramycin (Fig. S4B). Likewise, methyl-triclosan was unable to significantly reduce efflux pump activity (Fig. S5). These results support the conclusion that triclosan protonophore activity is required for the depletion of the tobramycin induced $\Delta\psi$ surge and inhibition of RND-type efflux pump activity.

ATP Depletion does not render cells more sensitive to tobramycin.

Another outcome of triclosan depleting the $\Delta\psi$ would be decreased energy generation, which could contribute to the sensitivity of biofilms to tobramycin. We performed antimicrobial susceptibility assays on 24-hr old biofilms grown in rich medium that were then DPBS-starved for 5 days. We observed the same synergy of the combination in these conditions as treatment with triclosan or tobramycin alone failed to cause bacterial killing whereas the combination of triclosan and tobramycin caused significant killing (Fig. S6). These data suggest that the disruption of the $\Delta\psi$ by triclosan does not induce synergy by depletion of ATP.

Triclosan and tobramycin show enhanced efficacy in an *in vivo* wound model.

To determine if triclosan and tobramycin are more effective against biofilms *in vivo,* we tested their activity using a murine wound model (55, 56). In this model, a 1-day old wound on the back of SKH-1 hairless mice were infected with ~$1x10^9$ XEN 41 bioluminescent *P. aeruginosa* cells growing as biofilms to allow imaging of the infection using the In Vivo Imaging System.

293 2-day old biofilms were treated for 4-hrs using an agarose hydrogel imbedded with either
294 triclosan or tobramycin alone or in combination. Triclosan hydrogels had no effect compared to
295 control hydrogels while tobramycin hydrogels resulted in statistically non-significant 2.5-fold-
296 reduction in bioluminescence (Fig. 6). Hydrogels embedded with triclosan and tobramycin
297 resulted in statistically significant 4.5-fold-reduction in bioluminescence. The combination
298 hydrogels resulted in greater than 4-fold reduction in five mice whereas tobramycin treatment
299 only achieved this level of killing once.
300

301 **Discussion**

302 Here we report that triclosan acts as a protonophore uncoupler against *P. aeruginosa*
303 growing as biofilms (34-38). To our knowledge, this is the first report of protonophore activity
304 by triclosan against Gram-negative bacteria growing as biofilms both *in vitro* and *in vivo*.
305 Adaptive resistance, occurring within 2-hrs of exposure, reduces accumulation of
306 antimicrobials by inducing the activity of PMF driven RND-type efflux pumps and alterations to
307 the OM (8-12) . We previously demonstrated classic aminoglycoside adaptive resistance, finding
308 *P. aeruginosa* biofilms were refractory to tobramycin killing until ~6-hrs, with the greatest
309 resistance observed at 2-hrs. However, the addition of triclosan with tobramycin led to rapid
310 killing of *P. aeruginosa* biofilms (28). Here we show that triclosan reduces the activity of PMF
311 driven RND-type efflux pumps, resulting in greater tobramycin accumulation within cells (Figs.
312 3 and 4). Triclosan does this by inhibiting a tobramycin induced surge in $\Delta\psi$ occurring at 2-hrs
313 (Fig. 5). Together, our past and present data suggest that the disruption of the $\Delta\psi$ depletes the
314 energy required for effective efflux pump mediated adaptive resistance (Fig. 7) (28). In support
315 of this model, methyl-triclosan, which lacks a dissociable proton and thus cannot act as

316 protonophore, was completely ineffective alone and in combination with tobramycin (Figs. S3-
317 5).

318 In addition to protein-specific corruption of translation at ribosomes, the very process of
319 aminoglycoside uptake augments its bactericidal activity by non-specifically disrupting the OM
320 and IM (18-20). In the first step of uptake, positively charged aminoglycosides bind to the
321 negative charged components of the OM, including lipopolysaccharide and phospholipids in
322 Gram-negative bacteria. This is followed by the displacement of magnesium ions responsible for
323 OM stabilization, promoting uptake by disrupting and increasing OM permeability (18-20). In
324 addition, aminoglycosides can diffuse through porins in the OM (18-20). In EDP-I,
325 aminoglycosides cross the IM via a mechanism that is influenced by the PMF, specifically the
326 $\Delta\psi$, in a concentration dependent manner (18-20). In EDP-II, aminoglycoside cause the
327 mistranslation of proteins by membrane associated ribosomes, resulting in the insertion of
328 misfolded proteins in the IM, which permeabilizes the cytoplasmic membrane accelerating its
329 own accumulation (18-20).

330 Several studies have shown that aminoglycoside-mediated killing of bacteria can be
331 enhanced by supplementing exogenous metabolites or host derived molecules, which increase
332 cellular respiration, PMF, and the uptake of aminoglycosides through EDP-I (57-62). However,
333 these studies used aminoglycoside concentrations ranging from 2-25 μg/mL on cells growing
334 planktonically (57-62). Alternatively, the experiments described here used 250 μg/mL of
335 tobramycin on *P. aeruginosa* biofilms. This higher concentration of tobramycin is more
336 clinically relevant and similar to antipseudomonal therapeutic dosing in cystic fibrosis patients
337 (1-3, 21, 22).

Although our model might appear to contradict these prior studies, it has been demonstrated that at concentrations of aminoglycosides greater than 30 μg/mL, as used here, the PMF is less important for aminoglycoside uptake during EDP-I (18-20). In fact, we observed that 250 μg/mL tobramycin can ultimately lead to biofilm killing at 24-hrs similar to the combination, suggesting that slow uptake of tobramycin during the EDP-I phase in the absence of triclosan eventually permeabilizes the IM stimulating EDP-II uptake in most of the biofilm (Fig. S7) (4, 48). However, the addition of triclosan accelerates this process by uncoupling the PMF such that maximal killing occurs at 4-hrs, as previously described (Fig. S7) (28). Together, our results support a model where triclosan reduction of the $\Delta\psi$ reduces the PMF required for active efflux leading to rapid accumulation of tobramycin in the cytoplasm and the stimulation of EDP-II uptake, which triggers irreversible cytosolic tobramycin accumulation and cell killing (4). In support of our model, other publications have demonstrated that bacteria can be sensitized to antibiotics by molecules that dissipate the PMF (24-27, 63-66). Specifically, Verstraeten et al., found that depleting the $\Delta\psi$ by overexpressing Obg in *E. coli* increased intercellular accumulation of tobramycin, likely through reduced efflux (65).

RND-type efflux pumps are intricately linked to antibiotic resistance, especially in biofilms (4, 54, 67). RND-type efflux pumps consist of three proteins which span the inner membrane and outer membrane (Fig. 7) (54). The inner membrane protein (IMP, e.g. MexX) catalyzes the H^+ dependent efflux of compounds and provides antimicrobial specificity whereas the periplasmic membrane fusion protein (MFP, e.g. MexY) connects the outer membrane protein (OMP, e.g. OprM) to the IMP creating an exit channel (54). There are 12 RND-type efflux pumps encoded in the genome of *P. aeruginosa* (4) and five are well characterized: MexAB-OprM, MexCD-OprJ, MexEF-OprN, MexXY-OprM and MexJK-OpRM (4). In

361 particular, the MexXY-OprM pump is responsible for aminoglycoside efflux, playing an
362 essential role in adaptive and acquired resistance (9-12, 68). The most frequent class of
363 aminoglycoside resistant mutants in CF isolates of *P. aeruginosa* have lost function of the
364 repressor MexZ, leading to overproduction of the RND-type efflux pump MexXY (67, 69). We
365 previously demonstrated that the combination of tobramycin and triclosan exhibited significant
366 killing against a clinical CF *P. aeruginosa* isolate AMT0023_34 that is tobramycin resistant by
367 such a mechanism (28). Importantly, our results suggest that the triclosan addition can potentiate
368 tobramycin to treat *P. aeruginosa* infections that are tobramycin resistant due to the
369 overexpression of efflux pumps. Which of the multiple efflux pumps impacted by triclosan
370 addition is under investigation.

371 We show that triclosan reduces efflux pump activity through the reduction of the $\Delta\psi$, but
372 this activity does not potentiate the cells to triclosan itself, even though the RND-type efflux
373 pump TriABC is a triclosan resistance mechanism expressed by *P. aeruginosa* (31). We
374 hypothesize that although triclosan reduces efflux pump activity, this reduction is not sufficient
375 to render *P. aeruginosa* sensitive to triclosan because this species also encodes the triclosan
376 resistant FabI ortholog FabV (30). In addition, if triclosan reduces efflux pump activity, one may
377 predict it should broadly enhance multiple classes of antibiotics (70). However, our prior study
378 demonstrated that triclosan only enhanced aminoglycosides and to a lesser extent, tetracycline
379 (28). Because triclosan does not completely abolish the $\Delta\psi$, we hypothesize that triclosan only
380 enhances antibiotic killing by bacteria that are known to trigger adaptive resistance through
381 disrupting translation, such as aminoglycosides and tetracyclines (8-10, 12-15).

382 *P. aeruginosa* encodes two genes for elongation factor G (EF-G), *fusA1* and *fusA2* (71).
383 *In vitro* translation studies have suggested that *fusA2* is the primary EF-G responsible for

384 ribosome translocation while the function of *fusA1* remains unclear (71). *fusA1* and *fusA2* are
385 98% similar and 84% identical, but interestingly *fusA1* expression is induced in cells growing as
386 biofilms compared to cells growing planktonically (72). Recently, a new tobramycin resistance
387 mechanism caused by mutations in *fusA1* has been identified in CF *P. aeruginosa* isolates (73).
388 In fact, one of the mutations that we report here, L40Q, was identified in clinical isolates (73).
389 These results support our findings that mutations in *fusA1* reduce susceptibility to
390 aminoglycosides through an unknown mechanism(s).

391 In addition to mutations in the gene *fusA1*, all resistant mutants had SNPs or deletions in
392 the previously described genes *ptsP*, involved in the overproduction of the phenazine pyocyanin
393 responsible for the generation of reactive oxygen species (74), *mexT*, a repressor of the RND-
394 type efflux pump MexEF-OprN (75), and *wspF*, a regulatory of the diguanylate cyclase WspR
395 (76-78) (Table 1). Mutations in *mexT* were deletions or the SNP P170L (Table 1). These
396 mutations and deletions likely result in the overexpression of the RND-type efflux pump
397 MexEF-OprN due to loss of repression by MexT (75). This finding supports our model that the
398 inhibition of efflux pump activity by triclosan drives increased tobramycin accumulation and
399 activity. It is unclear what benefits would be provided by increased pyocyanin production, a
400 quorum sensing controlled metabolite that is toxic and plays numerous roles in *P. aeruginosa*
401 physiology and virulence (79). There is evidence to suggest pyocyanin may restrict social
402 cheating in biofilms and promote tolerance to oxidative stress, which may provide some
403 tolerance to tobramycin and triclosan treatment (80). Mutations in *wspF* are not surprising as
404 these promote the formation of highly tolerant biofilms by increasing intracellular cyclic di-GMP
405 stimulating increased EPS production that reduces the diffusion of tobramycin (76-78).

406 Owing to decades of overuse, the FDA has restricted the use of triclosan due to concerns
407 over bioaccumulation and the potential for induction of resistance to other antibiotics in bacteria.
408 However, triclosan maintains FDA approval for use in Colgate® total toothpaste at 100-times the
409 concentrations used in this study. In support of this decision, numerous toxicity studies and the
410 Scientific Committee on Consumer Safety published by the European Union has found that
411 triclosan is safe when used appropriately (40-42). Furthermore, envisioning triclosan as an
412 adjuvant for tobramycin therapy for CF, we previously performed acute and long-term triclosan
413 toxicity studies in rats and showed that direct delivery of triclosan to lungs did not elicit
414 significant toxicity (28).

415 More broadly, our results suggest that protonophores could be potent antibiotic adjuvants
416 that enhance antibiotic killing against bacterial biofilms. Protonophores are being developed as
417 novel antibiotics to target *Mtb*. Specifically, diphenyl ethers such as SQ109 are in phase II
418 clinical trials in humans (24-27, 64). Moreover, a HTS recently identified that the c-Jun N-
419 terminal kinase inhibitor SU3327, renamed halicin, dissipates the ΔpH and PMF, demonstrating
420 growth inhibitory properties both *in vitro* and *in vivo* against several pathogens including some
421 multi-drug resistant strains (66). Importantly, protonophore uncouplers are already routinely used
422 for parasitic infections, including oxyclozanide, which we previously found synergizes with
423 tobramycin much like triclosan (39). In addition to protonophores functioning as antimicrobials,
424 there is also renewed interest in using these compounds to target such diseases as diabetes and
425 cancer, as well as slow aging, suggesting compounds with this activity are druggable targets
426 when used appropriately (81-83). Together, our results and other published studies demonstrate
427 that the use of protonophore uncouplers to target bacterial energetics is a promising new strategy
428 to target antimicrobial resistant infections (24).

Methods

Bacterial strains, culture conditions, and compounds.

All strains used in this study are listed in Table 1. Bacterial strains were grown in glass test tubes (18 X 150 mm) at 35ºC in cation adjusted Müeller-Hinton Broth II (MHB, Sigma-Aldrich) with agitation at 210 revolutions per minute (RPM). Antibiotics, methyl-triclosan, carbonyl cyanide 3-chlorophenylhydrazone (CCCP), and triclosan were obtained from Sigma-Aldrich. AFN-1252 was obtained from MedChemExpress. Tobramycin sulfate, gentamicin sulfate, and streptomycin sulfate were dissolved in autoclaved deionized water and filter sterilized using 0.22 µM filter membranes (Thomas Scientific). Triclosan was dissolved in 100% ethanol. Methyl-triclosan, CCCP, and AFN-1252 were dissolved in 100% dimethyl sulfoxide (DMSO).

Biofilm susceptibility testing using BacTiter-Glo™.

To measure the antimicrobial susceptibility of biofilms, the MBEC Assay® (Innovotech) was used as described (28). Briefly, an overnight culture was diluted and seeded into a MBEC plate in 10% MHB v/v diluted in DPBS and incubated for 24-hrs at 35ºC with agitation at 150 RPM. The MBEC lid was then washed to remove non-adherent cells, transferred to a 96-well treatment plate, and incubated for the indicated time at 35ºC without agitation. Following treatment, the MBEC lid was washed and transferred to a black 96-well ViewPlate (PerkinElmer) filled with 40% (v/v) BacTiter-Glo™ (Promega) diluted in DPBS to enumerate cell viability using luminescence by an EnVison Multilabel Plate Reader (PerkenElmer, Waltham, MA). The BacTiter-Glo™ Microbial Cell Viability Assay is a luminescent assay that determines the

451 number of viable cells based on quantification of ATP concentration. A calibration curve was
452 previously performed and it was found using a linear regression the coefficient of determination
453 was r^2=0.9884 for luminescence versus CFUs/mL (28).
454

455 **Selection for *P. aeruginosa* resistant mutants.**

456 To select mutants resistant to tobramycin and triclosan, we modified a protocol by
457 Lindsey and collages and serially passaged biofilms while treating them with ever increasing
458 concentrations of triclosan and tobramycin (Table S1) (44). 24-hr biofilms were formed as
459 described above and treated with triclosan and tobramycin for 24-hrs. After each treatment,
460 biofilms were sonicated for 15-mins (Branson Ultrasonics) to disperse surviving cells from the
461 pegs into 10% v/v MHB recovery media. Biofilms were then allowed to re-form on new pegs
462 overnight. The next day, passaged biofilms were treated at a slightly higher concentration of
463 triclosan and tobramycin. Following the treatment, the recovery process was repeated, and
464 biofilms were re-formed. We split the treatment groups into three regimens: gradual, moderate
465 and sudden (Table S1). The gradual treatment group was initially treated with 0.4 µM of
466 triclosan and 0.004 µM of tobramycin, which is 250x less than the MIC of tobramycin (28). The
467 moderate treatment group was initially treated with 8 µM of triclosan and 0.08 µM of
468 tobramycin, which is 12.5x less than the MIC of tobramycin (28). And then the two treatment
469 groups were treated in subsequent cycles with ever increasing concentrations of triclosan and
470 tobramycin at the same rate. The sudden treatment series was treated with 500 µM of triclosan
471 and tobramycin from cycle day 1 and was eradicated. By serially passaging biofilms and
472 gradually increasing the concentration of triclosan and tobramycin, two resistant mutant
473 populations were established, 30_B2 and 30_F1 (Cycle_Location on 96-well plate). Each mutant

pool was then streaked on LB agar plates for single colony isolation, and 96 single colony mutants were isolated from each plate, totaling 192 single colony mutants.

Whole genome sequencing.

Genomic deoxyribonucleic acid (gDNA) was isolated from each mutant using the Wizard® gDNA purification kit (Promega). Illumina NextSeq was then performed by the Genomic Services Facility at Indiana University Center for Genomics and Bioinformatics. To identify single nucleotide polymorphisms (SNPs), sequencing results were first verified for quality using FASTQC and aligned to the PAO1 reference genome (84), which can be downloaded from the *Pseudomonas* Genome Database (http://www.pseudomonas.com) using the *Breseq* pipeline, which can be downloaded from (http://barricklab.org) (85). All identified SNPs are listed in the supplemental spreadsheet.

Ethidium bromide efflux pump assay.

Intercellular accumulation of ethidium bromide, which is a substrate for RND-type efflux pumps, was measured fluorometrically as previously described (49, 86). As described above, 24-hr old biofilms were formed in 96-well black ViewPlate. 10 µg/mL of ethidium bromide was added to each well along with various treatments. Fluorescence was recorded every 2-hrs for 6-hrs using a SpectraMax M5 microplate spectrophotometer system ($\lambda_{excite}/\lambda_{emit}$ 530/600 nm).

494 **BacLight™ membrane potential assay and cell permeabilization assay.**

495 To measure changes in membrane potential and cellular permeabilization the BacLight™
496 Membrane Potential Assay was used in combination with the cell impermeable live/dead TO-
497 Pro™-3 iodide stain, as previously described (39). Briefly, 24-hr old biofilms were formed in
498 glass test tubes (18 x 150 mm) in 1 mL of 10% (v/v) MHB at 35°C and agitated at 150 RPM.
499 Cells were washed in DPBS to remove non-adherent cells and treated with triclosan and
500 tobramycin for 2-hrs. Following treatment, cells were washed in DPBS (without magnesium and
501 calcium), and the biofilm was disrupted from the air-liquid interface. The cells were stained in 1
502 mL of DPBS for 5-mins with DiOC2(3). This dye emits in the fluorescein isothiocyanate (FITC)
503 channel within all cells. However, greater membrane potential drives accumulation and stacking
504 of the dye in the cell cytoplasm, shifting emission to the phycoerythrin (PE) channel. TO-
505 PRO™-3 iodide, which emits in the allophycocyanin (APC) channel, was used to identify
506 permeabilized cells, which fluoresces in cells that have compromised membranes by
507 intercalating DNA. Single cell flow cytometry was performed on an LSR II (BD Biosciences),
508 with excitation from 488 mm and 640 mm lasers, and analyzed in FITC/PE and APC channels,
509 respectively.
510

511 **Tobramycin accumulation and extrusion assay.**

512 To measure the accumulation of tobramycin within cells in biofilms, tobramycin was
513 conjugated to Texas red (Sigma-Aldrich) using an amine conjugation reaction, as previously
514 described (50). Briefly, one milligram of Texas Red sulfonyl chloride (Thermo Fisher Scientific)
515 was resuspended in 50 µL of anhydrous N,N-dimethylformamide (Sigma-Aldrich) on ice. The

516 solution was added slowly to 2.3 mL of 100 mM K2CO3 at pH 8.5, with or without 10 mg/mL
517 tobramycin (Sigma-Aldrich), on ice. Conjugated tobramycin was used at a concentration of 250
518 µg/mL (~500 µM) alone and in combination with 100 µM of triclosan against 24-hr old biofilms
519 formed in glass test tubes at the air-liquid interface, as described above. Following treatments,
520 biofilms were washed in DPBS and then disrupted with autoclaved wooden sticks into 1 mL of
521 0.2% Triton X-100 to lyse cells (Sigma-Aldrich). Lysed cells were then transferred to
522 spectrophotometer cuvettes (Thermo Fisher Scientific) and read using a SpectraMax M5
523 microplate spectrophotometer system ($\lambda_{excite}/\lambda_{emit}$ 595/615 nm). Extrusion assays were performed
524 in a similar fashion, except after 30-mins of treatment, biofilms were washed three times in
525 DPBS and then allowed to recover in treatment-free 1% MHB media for 30-mins. After
526 recovery, the media was read as described above.
527

528 **DPBS-starved *P. aeruginosa* biofilms.**

529 24-hr old biofilms were formed on MBEC™ plates as described above. After 24-hrs, the
530 lid was washed for 5-mins to remove non-adherent cells, transferred to a 96-well plate containing
531 DPBS, and incubated at 35ºC with agitation at 150 RPM for 5-days.
532

533 **Agarose hydrogels.**

534 Agarose hydrogels were made as previously described (56). Briefly, by dissolving 1 gm
535 of agarose (Sigma-Aldrich) into 200 mL of Tris-acetate-EDTA (TAE) buffer and heated to form
536 a homogenous solution using a microwave. The 0.5% agarose solution was then allowed to cool
537 and various treatments were added. The solution was then poured into 100 x 15 mm petri dishes

(Thermo Fisher Scientific) and stored at 4°C overnight. Prior to treatment, a 4 mm biopsy punch (VWR) was used to create hydrogel wafers.

Murine wound infection model.

Wound surgery was performed on 8-9 week-old male and female SKH-1 mice (Charles River) and infected with a bioluminescent derivative of PAO1, Xen41 (PerkinElmer), which constitutively expresses *luxCDABE* gene, as previously described with the following modifications (55, 56). Briefly, 24-hr old biofilms were formed on sterilized polycarbonate membrane filters with a 0.2 µM pore size (Millipore Sigma) by diluting an overnight culture to an OD_{600} of 0.001 and pipetting 100 µl on 4 membranes on a tryptic soy agar (TSA) plate. 24-hr old biofilms were scrapped using L-shaped spreaders (Sigma-Aldrich) from each membrane and re-suspended in 500 µl of DPBS. 20 µl of the biofilm-suspension was inoculated into the 24-hr old wounds previously formed on the dorsal side of the mouse midway between the head and the base of the tail. 24-hrs later the biofilm within the wound was imaged using *in vivo* imaging system (IVIS) (Perkin Elmer). Then the biofilm was treated by placing a 4 mm 0.5% agarose hydrogel wafer either containing various treatments or only being made up of agarose alone on top of the wound. To quantify antimicrobial activity, the wound was then imaged 4-hrs later using IVIS and total flux (p/s) in radiance was used to quantify bacterial susceptibility. The loss of radiance indicates fewer cells are present within the wound. Vertebrate research was approved by the Michigan State University Institutional Animal Care and Use Committee application 03/18-036-00.

Statistics

Significance was determined as described in accompanying figure legends by either a one-way ANOVA or two-way ANOVA followed by Sidak's or Bonferroni's multiple comparisons posttest, respectively. Unpaired t-test were also used as described in accompanying figure legends. The "n" indicates the number of biological replicates. For murine wound infection experiments, sample sizes were determined based on preliminary studies using groups that were sufficient to achieve a desired power of 0.85 and an alpha value of 0.05. All analyses were performed using GraphPad Prism version 8.4.1 (San Diego, CA) and a p-value of < 0.05 was considered statistically significant.

Acknowledgments

This work was supported by grants from the Hunt for a Cure Foundation, the NSF BEACON center for evolution in action (DBI-0939454), NIH grants GM109259, GM110444, and AI143098 to C.M.W. and the Cystic Fibrosis Foundation Traineeship to M.M.M. In addition, M.M.M. was supported by a Wentworth Fellowship and Rudolf Hugh award from the MSU Department of Microbiology and Molecular Genetics and by a Dissertation Completion Fellowship from the College of National Science. We thank both Sandra O'Reilly and Louis King of the Michigan State Research Technology Support Facility for their assistance in the wound model and flow cytometry experiments, respectively. We also thank the Genomic Services Facility at Indiana University Center for Genomics and Bioinformatics. And we thank Lucas Demey, Mitchell Zachos and Emily Horning for their technical assistance.

582 **Table**

583

584 **Table 1. Bacterial strains used in this study.**

Strain	Characteristics	Reference
PAO1	*P. aeruginosa* Standard Reference Strain	(28)
Xen41	Bioluminescent PAO1 derivative: constitutively expresses *luxCDABE* gene	PerkinElmer
30_F1_5	*fusA1*, L40Q (C**T**G→C**A**G) *wspF*, Q132* (CAG→TAG) *PtsP*, A718P (**G**CC→**C**CC) *mexT*, P170L (C**C**G→C**T**G)	This Study
30_F1_6	*fusA1*, L40Q (C**T**G→C**A**G) *wspF*, Q132* (CAG→TAG) *PtsP*, coding (703/2280 nt) *mexT*, coding (58-137/1044 nt)	This Study
30_B2_8	*fusA1*, T64A (**A**CC→**G**CC) *wspF*, Q132* (CAG→TAG) *PtsP*, coding (703/2280 nt) *mexT*, coding (58-137/1044 nt)	This Study
30_B2_30	*fusA1*, T64A (**A**CC→**G**CC) *wspF*, Q132* (CAG→TAG) *PtsP*, A718P (**G**CC→**C**CC) *mexT*, P170L (C**C**G→C**T**G)	This Study
30_B2_57	*fusA1*, T64A (**A**CC→**G**CC) *wspF*, Q132* (CAG→TAG) *PtsP*, coding (703/2280 nt) *mexT*, coding (58-137/1044 nt)	This Study
30_B2_82	*fusA1*, T64A (**A**CC→**G**CC) *wspF*, Q132* (CAG→TAG) *PtsP*, A718P (**G**CC→**C**CC) *mexT*, P170L (C**C**G→C**T**G)	This Study

585 All additional SNPs in evolution mutants are listed in the supplemental spreadsheet.

586

Figure legends

FIG 1. Triclosan in combination with tobramycin results in increased permeabilization of cells within biofilms. 24-hr old biofilms were treated with triclosan (100 µM), or tobramycin (500 µM), alone and in combination for 2-hrs. Cells were stained with the live/dead cell indicator TO-PRO™-3 iodide to determine the number of cells that were permeabilized. The results are percent averages plus the standard error mean (SEM, n=4). Percent values indicate the average relative abundance of events within each gate normalized to the total number of events analyzed, excluding artifacts, aggregates and debris. A one-way analysis of variance (ANOVA) followed by Sidak's multiple comparison post-hoc test was used to determine statistical significance between each treatment and the untreated control or tobramycin treatment alone with the combination treatment. *, $p<0.05$. NS, not significant.

FIG 2. Mutants from experimental evolution are resistant to tobramycin and the combination. 24-hr old biofilms were treated with triclosan (100 µM) and tobramycin (500 µM) alone and in combination. The results represent the means plus SEM (n=6). A two-way ANOVA followed by Bonferroni's posttest was used to determine statistical significance between each treatment and the untreated control. *, $p<0.05$. NS, not significant.

FIG 3. Triclosan reduces the activity of RND-type efflux pumps. 24-hr biofilms were stained with ethidium bromide to measure accumulation. Biofilms were treated with CCCP (100 µM), triclosan (100 µM), tobramycin (500 µM) alone and in combination. Fluorescence was read at 0,2,4, and 6-hrs. Results represent the average arbitrary fluorescence units ±SEM (n=6).

FIG 4. Triclosan results in increased cellular accumulation and extrusion of Texas Red conjugated tobramycin (TbTR). 24-hr old biofilms grown in glass test tubes were treated for 30-mins with triclosan (100 µM), CCCP (100 µM) and TbTR (250 µg/mL). (A) Then cells were disrupted from the biofilms and lysed with 0.2% Triton-X 100® to measure intercellular accumulation of TbTR. (B) To measure extrusion, biofilms were first treated for 30-mins and washed three-times in DPBS. Biofilms then recovered in treatment free media for 30-mins and fluorescence of the media was measured. TbTR was measured by relative fluorescence units using excitation 595_{nm} and emission 615_{nm}. Results represent the average arbitrary fluorescence units ±SEM (n=6). For panel A, a One-Way-ANOVA was performed comparing TbTR alone vs CCCP and TbTR and vs triclosan and TbTR. For panel B, an unpaired t-test was performed comparing TbTR versus triclosan and TbTR. *, $p<0.05$. NS, not significant.

FIG 5. Triclosan reduces the membrane potential surge induced by tobramycin at 2-hours. 24-hr old biofilms were treated with triclosan (100 µM), or tobramycin (500 µM), alone and in combination for 2-hrs. Cells were stained with DiOC2(3) to measure the membrane potential. Dead or permeabilized cells were excluded from membrane potential analysis by parallel staining with the dead cell indicator TO-PRO™-3 iodide. The results are percent averages plus the SEM (n=4). Percent values indicate the average relative abundance of events within each gate normalized to the total number of events analyzed, excluding dead cells, artifacts, aggregates and debris. A one-way ANOVA followed by Sidak's multiple comparison post-hoc test was used to determine statistical significance between each treatment and the untreated control, and tobramycin treatment alone was compared with the combination. *, $p<0.05$. NS, not significant.

FIG 6. Triclosan and tobramycin hydrogels are more effective than tobramycin hydrogels in a murine wound model. 24-hr old bioluminescent biofilms formed within wounds were treated with triclosan (100 µM), or tobramycin (400 µM), alone and in combination for 4-hrs in a hydrogel. Reduction in the number of cells within biofilms was quantified using IVIS. The results are fold reduction of three separate experiments ±SEM, no treatment n=6, triclosan n=6, tobramycin n=10, triclosan and tobramycin n=9. A one-way ANOVA followed by Bonferroni's multiple comparison post-hoc test was used to determine statistical significance between each treatment and the untreated control and tobramycin treatment alone was compared with tobramycin and triclosan (*, $p<0.05$).

FIG 7. Triclosan sensitizes *P. aeruginosa* to tobramycin by acting as a protonophore, inhibiting efflux pump activity, and abolishing adaptive resistance. (1) Within 2-hrs of exposure to tobramycin, adaptive resistance occurs, (2) which is due to the induction of RND-type efflux pumps and surge in membrane potential ($\Delta\psi$), resulting in reduced accumulation of tobramycin within the cytosol. (3) Triclosan shuttles protons across the inner membrane, collapsing the proton motive force (Δp) and depolarizing the $\Delta\psi$. Consequently, efflux pump activity is reduced and there is enhanced accumulation of tobramycin within the cytosol. Finally, tobramycin binds to the A-site of the ribosome, corrupting protein synthesis and causing membrane permeabilization. Overall, triclosan accelerates and increase the effectiveness of tobramycin by reducing the $\Delta\psi$ and efflux pump activity. Proton gradient, ΔpH. Outer membrane protein (OMP), membrane fusion protein (MFP), inner membrane protein (IMP).

Supplemental Figure Legends

FIG S1. AFN-1252 alone or in combination with tobramycin is not effective against mature biofilms. 24-hr old biofilms grown on MBEC plates were treated for 6-hrs with AFN-1252 (400 µM), tobramycin (400 µM), alone and in combination in two-fold dilutions, and the number of viable cells within the biofilms were quantified by BacTiter-Glo^{TM}. The assay was performed twice in in duplicate. The results represent means ± the Standard Error Mean (SEM). A one-way analysis of variance (ANOVA) followed by Bonferroni's multiple comparison post-hoc test was used to determine statistical significance between tobramycin versus the combination (NS, not significant).

FIG S2. Initial tobramycin treatment is required for the combination to be effective. 24-hr old biofilms grown on MBEC plates were treated sequentially. First, biofilms were treated for 3-hours with tobramycin (500 µM) and then washed three times in DPBS for 3-mins each, before being treated with triclosan (100 µM) for 3-hours or vice versa. As a control, biofilms were also treated for 6-hrs with triclosan and tobramycin. The number of viable cells within the biofilms were quantified by BacTiter-Glo^{TM}. The assay was performed twice in in duplicate. The results represent means plus the SEM. A one-way ANOVA followed by Bonferroni's multiple comparison post-hoc test was used to determine statistical significance between each treatment and the untreated control. *, $p<0.05$. NS, not significant.

FIG S3. Methyl-triclosan alone or in combination with tobramycin is not effective against mature biofilms. 24-hr old biofilms grown on MBEC plates were treated for 6-hrs with methyl-triclosan (100 µM), tobramycin (400 µM), alone and in combination in two-fold dilutions, and

679 the number of viable cells within the biofilms were quantified by BacTiter-Glo™. The assay was
680 performed twice in in duplicate. The results represent means ±SEM. A one-way ANOVA
681 followed by Bonferroni's multiple comparison post-hoc test was used to determine statistical
682 significance compared to tobramycin alone and the combination. NS, not significant.
683
684 **FIG S4. Methyl-triclosan alone and in combination with tobramycin does not reduced the**
685 **surge in membrane potential induced by tobramycin at 2-hours.** 24-hr old biofilms were
686 treated with methyl-triclosan (100 µM), or tobramycin (500 µM), alone and in combination for
687 2-hrs. Cells were stained with DiOC2(3) and TO-PRO™-3 iodide to determine the number of
688 cells that maintained a membrane potential (A) or were permeabilized (B), respectively. Dead or
689 permeabilized cells were excluded from membrane potential analysis and are shown in panel B.
690 The experiment was performed two separate times in duplicate. The results are percent averages
691 plus the SEM. Percent values indicate the average relative abundance of events within each gate
692 normalized to the total number of events analyzed, excluding artifacts, aggregates and debris. A
693 one-way ANOVA followed by Sidak's multiple comparison post-hoc test was used to determine
694 statistical significance between each treatment and an untreated control, and tobramycin
695 treatment alone was compared with the combination. *, $p<0.05$, NS, not significant.
696
697 **FIG S5. Methyl-triclosan does not reduced RND-type efflux pump activity.** Ethidium
698 bromide is a substrate of RND-type efflux pumps. 24-hr biofilms were stained with ethidium
699 bromide to measure accumulation. Biofilms were treated with methyl-triclosan (100 µM) and
700 tobramycin (500 µM) alone and in combination. Fluorescence was read at 0,2,4, and 6-hrs. The

assay was performed three times in triplicate. Results represent the average arbitrary fluorescence units ±SEM.

FIG S6. DPBS starved biofilms are not more sensitive to tobramycin alone. 24-hour old biofilms were starved of nutrients by replacing media with DPBS for 5-days. Starved biofilms were treated with triclosan (100 µM), or tobramycin (500 µM), alone and in combination for 6-hrs. The number of viable cells within the biofilms was quantified using the BacTiter-Glo™ assay. The assay was performed once using three biological replicates. The results represent the means plus the SEM. A one-way ANOVA followed by Sidak's multiple comparison post hoc test was used to determine statistical significance between the combination treatment and the untreated control and between triclosan alone or tobramycin alone and the combination treatment as indicated by the bars. *, $P < 0.05$.

FIG S7. Tobramycin is as effective as the combination after 24-hrs of treatment. 24-hr old biofilms were treated for 24-hrs with triclosan (100 µM), tobramycin (500 µM), alone and in combination, and the number of viable cells within the biofilms were quantified by BacTiter-Glo™. The assay was performed at least three times in triplicate. The results represent means plus the SEM. A one-way ANOVA followed by Bonferroni's multiple comparison post-hoc test was used to determine statistical significance between untreated biofilms, tobramycin alone, and the combination treatment. In addition, using the same analysis, a comparison was made between tobramycin alone and the combination treatment. *, $P < 0.05$. NS, not significant. 4-hr treatments were previously published and are shown for comparison (28).

724 **References:**

725

726 1. Donlan RM, Costerton JW. Biofilms: survival mechanisms of clinically relevant
727 microorganisms. Clin Microbiol Rev. 2002;15(2):167-93.

728 2. O'Sullivan BP, Freedman SD. Cystic fibrosis. The Lancet. 2009;373(9678):1891-904.

729 3. Omar A, Wright JB, Schultz G, Burrell R, Nadworny P. Microbial Biofilms and Chronic
730 Wounds. Microorganisms. 2017;5(1):9.

731 4. Poole K. *Pseudomonas aeruginosa*: resistance to the max. Front Microbiol. 2011;2:65.

732 5. Livermore DM. Penicillin-binding proteins, porins and outer-membrane permeability of
733 carbenicillin-resistant and -susceptible strains of *Pseudomonas aeruginosa*. J Med Microbiol.
734 1984;18(2):261-70.

735 6. Morita Y, Tomida J, Kawamura Y. Responses of *Pseudomonas aeruginosa* to
736 antimicrobials. Front Microbiol. 2014;4.

737 7. Barclay ML, Begg EJ, Chambers ST, Thornley PE, Pattemore PK, Grimwood K. Adaptive
738 resistance to tobramycin in *Pseudomonas aeruginosa* lung infection in cystic fibrosis. J
739 Antimicrob Chemother. 1996;37(6):1155-64.

740 8. Hay T, Fraud S, Lau CH, Gilmour C, Poole K. Antibiotic inducibility of the *mexXY*
741 multidrug efflux operon of *Pseudomonas aeruginosa*: involvement of the MexZ anti-repressor
742 ArmZ. PLoS One. 2013;8(2):e56858.

743 9. Jeannot K, Sobel ML, El Garch F, Poole K, Plesiat P. Induction of the MexXY efflux pump
744 in *Pseudomonas aeruginosa* is dependent on drug-ribosome interaction. J Bacteriol.
745 2005;187(15):5341-6.

746 10. Hocquet D, Vogne C, El Garch F, Vejux A, Gotoh N, Lee A, et al. MexXY-OprM efflux
747 pump is necessary for a adaptive resistance of *Pseudomonas aeruginosa* to aminoglycosides.
748 Antimicrobial agents and chemotherapy. 2003;47(4):1371-5.

749 11. Karlowsky JA, Saunders MH, Harding GA, Hoban DJ, Zhanel GG. In vitro
750 characterization of aminoglycoside adaptive resistance in *Pseudomonas aeruginosa*. Antimicrob
751 Agents Chemother. 1996;40(6):1387-93.

752 12. Yamamoto M, Ueda A, Kudo M, Matsuo Y, Fukushima J, Nakae T, et al. Role of MexZ
753 and PA5471 in transcriptional regulation of *mexXY* in *Pseudomonas aeruginosa*. Microbiology.
754 2009;155(Pt 10):3312-21.

755 13. Barclay ML, Begg EJ. Aminoglycoside adaptive resistance: importance for effective
756 dosage regimens. Drugs. 2001;61(6):713-21.

14. Barclay ML, Begg EJ, Chambers ST. Adaptive resistance following single doses of gentamicin in a dynamic in vitro model. Antimicrob Agents Chemother. 1992;36(9):1951-7.

15. Barclay ML, Begg EJ, Chambers ST, Peddie BA. The effect of aminoglycoside-induced adaptive resistance on the antibacterial activity of other antibiotics against *Pseudomonas aeruginosa* in vitro. J Antimicrob Chemother. 1996;38(5):853-8.

16. Daikos GL, Lolans VT, Jackson GG. First-exposure adaptive resistance to aminoglycoside antibiotics in vivo with meaning for optimal clinical use. Antimicrob Agents Chemother. 1991;35(1):117-23.

17. Xiong YQ, Caillon J, Kergueris MF, Drugeon H, Baron D, Potel G, et al. Adaptive resistance of *Pseudomonas aeruginosa* induced by aminoglycosides and killing kinetics in a rabbit endocarditis model. Antimicrobial agents and chemotherapy. 1997;41(4):823-6.

18. Taber HW, Mueller JP, Miller PF, Arrow AS. Bacterial uptake of aminoglycoside antibiotics. Microbiol Rev. 1987;51(4):439-57.

19. Davis BD. Mechanism of bactericidal action of aminoglycosides. Microbiol Rev. 1987;51(3):341-50.

20. Hancock RE. Alterations in outer membrane permeability. Annu Rev Microbiol. 1984;38(1):237-64.

774 21. Mogayzel PJ, Jr., Naureckas ET, Robinson KA, Brady C, Guill M, Lahiri T, et al. Cystic
775 Fibrosis Foundation pulmonary guideline. pharmacologic approaches to prevention and
776 eradication of initial *Pseudomonas aeruginosa* infection. Ann Am Thorac Soc. 2014;11(10):1640-
777 50.

778 22. Chmiel JF, Aksamit TR, Chotirmall SH, Dasenbrook EC, Elborn JS, LiPuma JJ, et al.
779 Antibiotic management of lung infections in cystic fibrosis. I. The microbiome, methicillin-
780 resistant *Staphylococcus aureus*, gram-negative bacteria, and multiple infections. Ann Am Thorac
781 Soc. 2014;11(7):1120-9.

782 23. Brown ED, Wright GD. Antibacterial drug discovery in the resistance era. Nature.
783 2016;529(7586):336-43.

784 24. Hards K, Cook GM. Targeting bacterial energetics to produce new antimicrobials. Drug
785 Resist Updat. 2018;36:1-12.

786 25. Andries K, Verhasselt P, Guillemont J, Gohlmann HW, Neefs JM, Winkler H, et al. A
787 diarylquinoline drug active on the ATP synthase of *Mycobacterium tuberculosis*. Science.
788 2005;307(5707):223-7.

789 26. Hards K, Robson JR, Berney M, Shaw L, Bald D, Koul A, et al. Bactericidal mode of
790 action of bedaquiline. J Antimicrob Chemother. 2015;70(7):2028-37.

791 27. Feng X, Zhu W, Schurig-Briccio LA, Lindert S, Shoen C, Hitchings R, et al. Antiinfectives
792 targeting enzymes and the proton motive force. Proc Natl Acad Sci U S A. 2015;112(51):E7073-
793 82.

794 28. Maiden MM, Hunt AMA, Zachos MP, Gibson JA, Hurwitz ME, Mulks MH, et al.
795 Triclosan Is an Aminoglycoside Adjuvant for Eradication of *Pseudomonas aeruginosa* Biofilms.
796 Antimicrob Agents Chemother. 2018;62(6):e00146-18.

797 29. Heath RJ, Rubin JR, Holland DR, Zhang E, Snow ME, Rock CO. Mechanism of triclosan
798 inhibition of bacterial fatty acid synthesis. J Biol Chem. 1999;274(16):11110-4.

799 30. Zhu L, Lin J, Ma J, Cronan JE, Wang H. Triclosan resistance of *Pseudomonas aeruginosa*
800 PAO1 is due to FabV, a triclosan-resistant enoyl-acyl carrier protein reductase. Antimicrob Agents
801 Chemother. 2010;54(2):689-98.

802 31. Mima T, Joshi S, Gomez-Escalada M, Schweizer HP. Identification and characterization
803 of TriABC-OpmH, a triclosan efflux pump of *Pseudomonas aeruginosa* requiring two membrane
804 fusion proteins. J Bacteriol. 2007;189(21):7600-9.

805 32. Mitchell P. Coupling of phosphorylation to electron and hydrogen transfer by a chemi-
806 osmotic type of mechanism. Nature. 1961;191(4784):144-8.

807 33. Mitchell P. Chemiosmotic coupling in oxidative and photosynthetic phosphorylation.
808 1966. Biochim Biophys Acta. 2011;1807(12):1507-38.

809 34. Yoon DS, Choi Y, Cha DS, Zhang P, Choi SM, Alfhili MA, et al. Triclosan Disrupts SKN-
810 1/Nrf2-Mediated Oxidative Stress Response in C. elegans and Human Mesenchymal Stem Cells.
811 Sci Rep. 2017;7(1):12592.

812 35. Weatherly LM, Shim J, Hashmi HN, Kennedy RH, Hess ST, Gosse JA. Antimicrobial
813 agent triclosan is a proton ionophore uncoupler of mitochondria in living rat and human mast cells
814 and in primary human keratinocytes. J Appl Toxicol. 2016;36(6):777-89.

815 36. Popova LB, Nosikova ES, Kotova EA, Tarasova EO, Nazarov PA, Khailova LS, et al.
816 Protonophoric action of triclosan causes calcium efflux from mitochondria, plasma membrane
817 depolarization and bursts of miniature end-plate potentials. Biochim Biophys Acta Biomembr.
818 2018;1860(5):1000-7.

819 37. Teplova VV, Belosludtsev KN, Kruglov AG. Mechanism of triclosan toxicity:
820 Mitochondrial dysfunction including complex II inhibition, superoxide release and uncoupling of
821 oxidative phosphorylation. Toxicol Lett. 2017;275:108-17.

822 38. Ajao C, Andersson MA, Teplova VV, Nagy S, Gahmberg CG, Andersson LC, et al.
823 Mitochondrial toxicity of triclosan on mammalian cells. Toxicol Rep. 2015;2:624-37.

824 39. Maiden MM, Zachos MP, Waters CM. The ionophore oxyclozanide enhances tobramycin
825 killing of *Pseudomonas aeruginosa* biofilms by permeabilizing cells and depolarizing the
826 membrane potential. J Antimicrob Chemother. 2019;74(4):894-906.

827 40. Davison John SR, Maillard M, Pagès J-Y, Scenihr J-MO, et al. Scientific Committee on
828 Consumer Safety (SCCS): Opinion on triclosan antimicrobial resistance. DG Sanco Scientific
829 Committee on Consumer Safety. . 2010 22:1–56. .

830 41. Rodricks JV, Swenberg JA, Borzelleca JF, Maronpot RR, Shipp AM. Triclosan: a critical
831 review of the experimental data and development of margins of safety for consumer products. Crit
832 Rev Toxicol. 2010;40(5):422-84.

833 42. Fang JL, Stingley RL, Beland FA, Harrouk W, Lumpkins DL, Howard P. Occurrence,
834 efficacy, metabolism, and toxicity of triclosan. J Environ Sci Health C Environ Carcinog
835 Ecotoxicol Rev. 2010;28(3):147-71.

836 43. Rao KN, Lakshminarasimhan A, Joseph S, Lekshmi SU, Lau MS, Takhi M, et al. AFN-
837 1252 is a potent inhibitor of enoyl-ACP reductase from *Burkholderia pseudomallei*--Crystal
838 structure, mode of action, and biological activity. Protein Sci. 2015;24(5):832-40.

839 44. Lindsey HA, Gallie J, Taylor S, Kerr B. Evolutionary rescue from extinction is contingent
840 on a lower rate of environmental change. Nature. 2013;494(7438):463-7.

841 45. Pal C, Papp B, Lazar V. Collateral sensitivity of antibiotic-resistant microbes. Trends
842 Microbiol. 2015;23(7):401-7.

843 46. Rodnina MV, Savelsbergh A, Katunin VI, Wintermeyer W. Hydrolysis of GTP by
844 elongation factor G drives tRNA movement on the ribosome. Nature. 1997;385(6611):37-41.

845 47. Arnaud Bolard PPs, and Katy Jeannota. Mutations in Gene fusA1 as a Novel Mechanism
846 of Aminoglycoside Resistance in Clinical Strains of *Pseudomonas aeruginosa*. Antimicrobial
847 Agents and Chemotherapy. 2018;62(2):e01835-17.

848 48. Tseng BS, Zhang W, Harrison JJ, Quach TP, Song JL, Penterman J, et al. The extracellular
849 matrix protects *Pseudomonas aeruginosa* biofilms by limiting the penetration of tobramycin.
850 Environ Microbiol. 2013;15(10):2865-78.

851 49. Blair JM, Piddock LJ. How to Measure Export via Bacterial Multidrug Resistance Efflux
852 Pumps. mBio. 2016;7(4):e00840-16.

853 50. Sandoval R, Leiser J, Molitoris BA. Aminoglycoside antibiotics traffic to the Golgi
854 complex in LLC-PK1 cells. J Am Soc Nephrol. 1998;9(2):167-74.

855 51. Booth IR. The Regulation of Intracellular pH in Bacteria. Chichester, UK: John Wiley &
856 Sons, Ltd.; 2007. 19-37 p.

857 52. Campbell BD, Kadner RJ. Relation of aerobiosis and ionic strength to the uptake of
858 dihydrostreptomycin in *Escherichia coli*. Biochim Biophys Acta. 1980;593(1):1-10.

859 53. Paulsen IT, Brown MH, Skurray RA. Proton-dependent multidrug efflux systems.
860 Microbiol Rev. 1996;60(4):575-608.

861 54. Venter H, Mowla R, Ohene-Agyei T, Ma S. RND-type drug efflux pumps from Gram-
862 negative bacteria: molecular mechanism and inhibition. Front Microbiol. 2015;6:377.

863 55. Agostinho Hunt AM, Gibson JA, Larrivee CL, O'Reilly S, Navitskaya S, Needle DB, et al.
864 A bioluminescent *Pseudomonas aeruginosa* wound model reveals increased mortality of type 1
865 diabetic mice to biofilm infection. J Wound Care. 2017;26(Sup7):S24-S33.

866 56. Maiden MM, Zachos MP, Waters CM. Hydrogels Embedded With Melittin and
867 Tobramycin Are Effective Against *Pseudomonas aeruginosa* Biofilms in an Animal Wound
868 Model. Front Microbiol. 2019;10(1348):1348.

869 57. Allison KR, Brynildsen MP, Collins JJ. Metabolite-enabled eradication of bacterial
870 persisters by aminoglycosides. Nature. 2011;473(7346):216-20.

871 58. Barraud N, Buson A, Jarolimek W, Rice SA. Mannitol enhances antibiotic sensitivity of
872 persister bacteria in *Pseudomonas aeruginosa* biofilms. PLoS One. 2013;8(12):e84220.

873 59. Crabbe A, Ostyn L, Staelens S, Rigauts C, Risseeuw M, Dhaenens M, et al. Host
874 metabolites stimulate the bacterial proton motive force to enhance the activity of aminoglycoside
875 antibiotics. PLoS Pathog. 2019;15(4):e1007697.

876 60. Radlinski LC, Rowe SE, Brzozowski R, Wilkinson AD, Huang R, Eswara P, et al.
877 Chemical Induction of Aminoglycoside Uptake Overcomes Antibiotic Tolerance and Resistance
878 in *Staphylococcus aureus*. Cell Chem Biol. 2019;26(10):1355-64 e4.

879 61. Su YB, Peng B, Han Y, Li H, Peng XX. Fructose restores susceptibility of multidrug-
880 resistant *Edwardsiella tarda* to kanamycin. J Proteome Res. 2015;14(3):1612-20.

881 62. Su YB, Peng B, Li H, Cheng ZX, Zhang TT, Zhu JX, et al. Pyruvate cycle increases
882 aminoglycoside efficacy and provides respiratory energy in bacteria. Proc Natl Acad Sci U S A.
883 2018;115(7):E1578-E87.

884 63. Farha MA, Verschoor CP, Bowdish D, Brown ED. Collapsing the proton motive force to
885 identify synergistic combinations against *Staphylococcus aureus*. Chem Biol. 2013;20(9):1168-
886 78.

887 64. Foss MH, Pou S, Davidson PM, Dunaj JL, Winter RW, Pou S, et al. Diphenylether-
888 Modified 1,2-Diamines with Improved Drug Properties for Development against *Mycobacterium*
889 *tuberculosis*. ACS Infect Dis. 2016;2(7):500-8.

890 65. Verstraeten N, Knapen WJ, Kint CI, Liebens V, Van den Bergh B, Dewachter L, et al. Obg
891 and Membrane Depolarization Are Part of a Microbial Bet-Hedging Strategy that Leads to
892 Antibiotic Tolerance. Mol Cell. 2015;59(1):9-21.

893 66. Stokes JM, Yang K, Swanson K, Jin W, Cubillos-Ruiz A, Donghia NM, et al. A Deep
894 Learning Approach to Antibiotic Discovery. Cell. 2020;180(4):688-702 e13.

895 67. Piddock LJ. Clinically relevant chromosomally encoded multidrug resistance efflux pumps
896 in bacteria. Clin Microbiol Rev. 2006;19(2):382-402.

897 68. Morita Y, Tomida J, Kawamura Y. MexXY multidrug efflux system of *Pseudomonas*
898 *aeruginosa*. Front Microbiol. 2012;3(408):408.

899 69. Mena A, Smith EE, Burns JL, Speert DP, Moskowitz SM, Perez JL, et al. Genetic
900 adaptation of *Pseudomonas aeruginosa* to the airways of cystic fibrosis patients is catalyzed by
901 hypermutation. J Bacteriol. 2008;190(24):7910-7.

902 70. Askoura M, Mottawea W, Abujamel T, Taher I. Efflux pump inhibitors (EPIs) as new
903 antimicrobial agents against *Pseudomonas aeruginosa*. Libyan J Med. 2011;6.

904 71. Palmer SO, Rangel EY, Hu Y, Tran AT, Bullard JM. Two homologous EF-G proteins from
905 *Pseudomonas aeruginosa* exhibit distinct functions. PLoS One. 2013;8(11):e80252.

906 72. Anderson GG, Moreau-Marquis S, Stanton BA, O'Toole GA. In vitro analysis of
907 tobramycin-treated *Pseudomonas aeruginosa* biofilms on cystic fibrosis-derived airway epithelial
908 cells. Infect Immun. 2008;76(4):1423-33.

909 73. Bolard A, Plesiat P, Jeannot K. Mutations in Gene fusA1 as a Novel Mechanism of
910 Aminoglycoside Resistance in Clinical Strains of *Pseudomonas aeruginosa*. Antimicrob Agents
911 Chemother. 2018;62(2).

912 74. Xu H, Lin W, Xia H, Xu S, Li Y, Yao H, et al. Influence of ptsP gene on pyocyanin
913 production in *Pseudomonas aeruginosa*. FEMS Microbiol Lett. 2005;253(1):103-9.

914 75. Juarez P, Broutin I, Bordi C, Plesiat P, Llanes C. Constitutive Activation of MexT by
915 Amino Acid Substitutions Results in MexEF-OprN Overproduction in Clinical Isolates of
916 *Pseudomonas aeruginosa*. Antimicrob Agents Chemother. 2018;62(5).

917 76. D'Argenio DA, Calfee MW, Rainey PB, Pesci EC. Autolysis and autoaggregation in
918 *Pseudomonas aeruginosa* colony morphology mutants. J Bacteriol. 2002;184(23):6481-9.

919 77. Hickman JW, Tifrea DF, Harwood CS. A chemosensory system that regulates biofilm
920 formation through modulation of cyclic diguanylate levels. Proc Natl Acad Sci U S A.
921 2005;102(40):14422-7.

922 78. Starkey M, Hickman JH, Ma L, Zhang N, De Long S, Hinz A, et al. *Pseudomonas*
923 *aeruginosa* rugose small-colony variants have adaptations that likely promote persistence in the
924 cystic fibrosis lung. J Bacteriol. 2009;191(11):3492-503.

925 79. Lau GW, Hassett DJ, Ran H, Kong F. The role of pyocyanin in *Pseudomonas aeruginosa*
926 infection. Trends Mol Med. 2004;10(12):599-606.

927 80. Castaneda-Tamez P, Ramirez-Peris J, Perez-Velazquez J, Kuttler C, Jalalimanesh A,
928 Saucedo-Mora MA, et al. Pyocyanin Restricts Social Cheating in *Pseudomonas aeruginosa*. Front
929 Microbiol. 2018;9(1348):1348.

930 81. Barbosa EJ, Lobenberg R, de Araujo GLB, Bou-Chacra NA. Niclosamide repositioning
931 for treating cancer: Challenges and nano-based drug delivery opportunities. Eur J Pharm
932 Biopharm. 2019;141:58-69.

933 82. Chen W, Mook RA, Jr., Premont RT, Wang J. Niclosamide: Beyond an antihelminthic
934 drug. Cell Signal. 2018;41:89-96.

935 83. Childress ES, Alexopoulos SJ, Hoehn KL, Santos WL. Small Molecule Mitochondrial
936 Uncouplers and Their Therapeutic Potential. J Med Chem. 2018;61(11):4641-55.

937 84. Winsor GL, Griffiths EJ, Lo R, Dhillon BK, Shay JA, Brinkman FS. Enhanced annotations
938 and features for comparing thousands of *Pseudomonas* genomes in the *Pseudomonas* genome
939 database. Nucleic Acids Res. 2016;44(D1):D646-53.

940 85. Deatherage DE, Barrick JE. Identification of mutations in laboratory-evolved microbes
941 from next-generation sequencing data using breseq. Methods Mol Biol. 2014;1151:165-88.

942 86. Olmsted J, 3rd, Kearns DR. Mechanism of ethidium bromide fluorescence enhancement
943 on binding to nucleic acids. Biochemistry. 1977;16(16):3647-54.

944

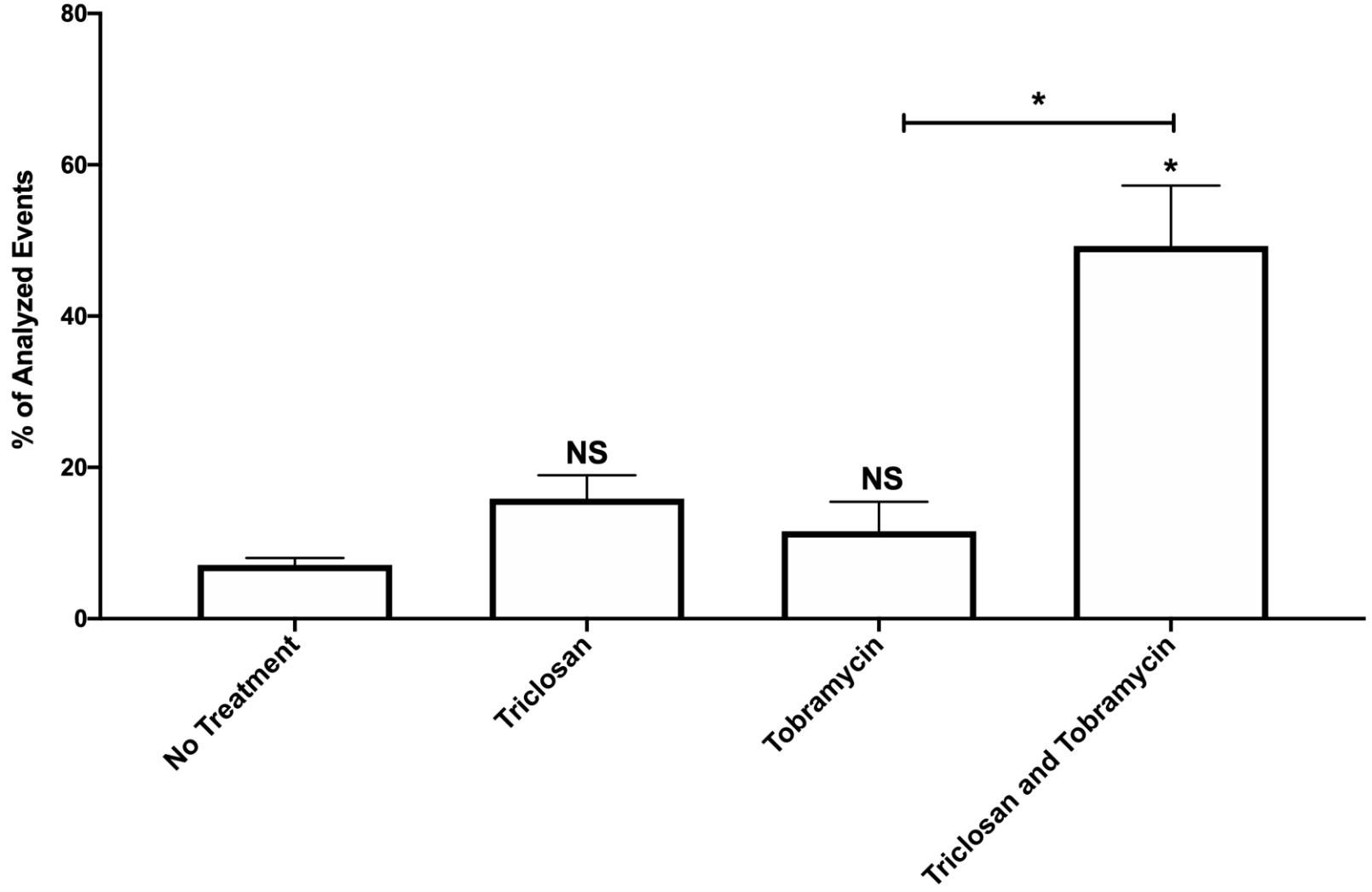

FIG 1. Triclosan in combination with tobramycin results in increased permeabilization of cells within biofilms. 24-hr old biofilms were treated with triclosan (100 µM), or tobramycin (500 µM), alone and in combination for 2-hrs. Cells were stained with the live/dead cell indicator TO-PRO™-3 iodide to determine the number of cells that were permeabilized. The results are percent averages plus the standard error mean (SEM, n=4). Percent values indicate the average relative abundance of events within each gate normalized to the total number of events analyzed, excluding artifacts, aggregates and debris. A one-way analysis of variance (ANOVA) followed by Sidak's multiple comparison post-hoc test was used to determine statistical significance between each treatment and the untreated control or tobramycin treatment alone with the combination treatment. *, $p<0.05$. NS, not significant.

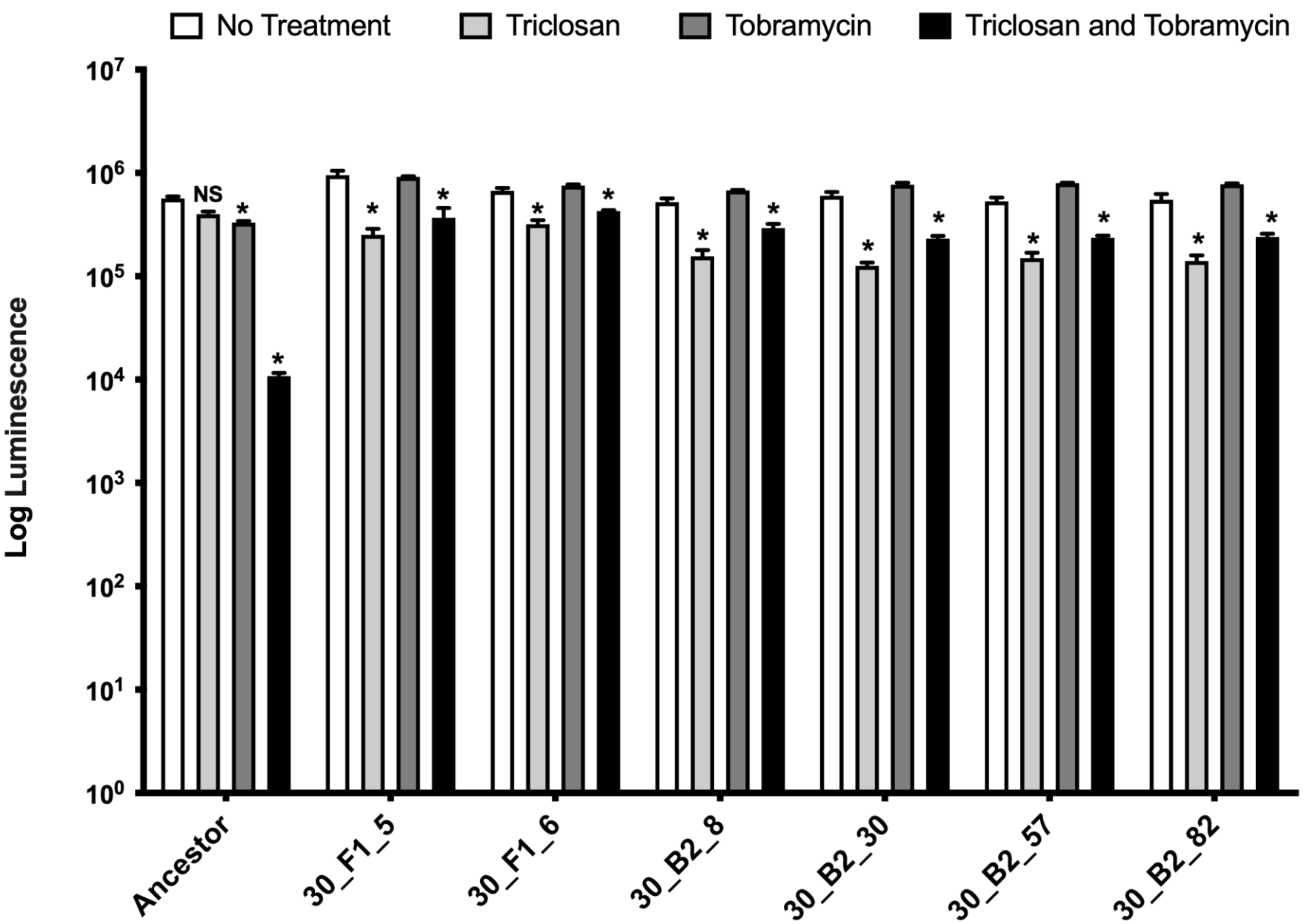

FIG 2. Mutants from experimental evolution are resistant to tobramycin and the combination. 24-hr old biofilms were treated with triclosan (100 µM) and tobramycin (500 µM) alone and in combination. The results represent the means plus SEM (n=6). A two-way ANOVA followed by Bonferroni's posttest was used to determine statistical significance between each treatment and the untreated control. *, $p<0.05$. NS, not significant.

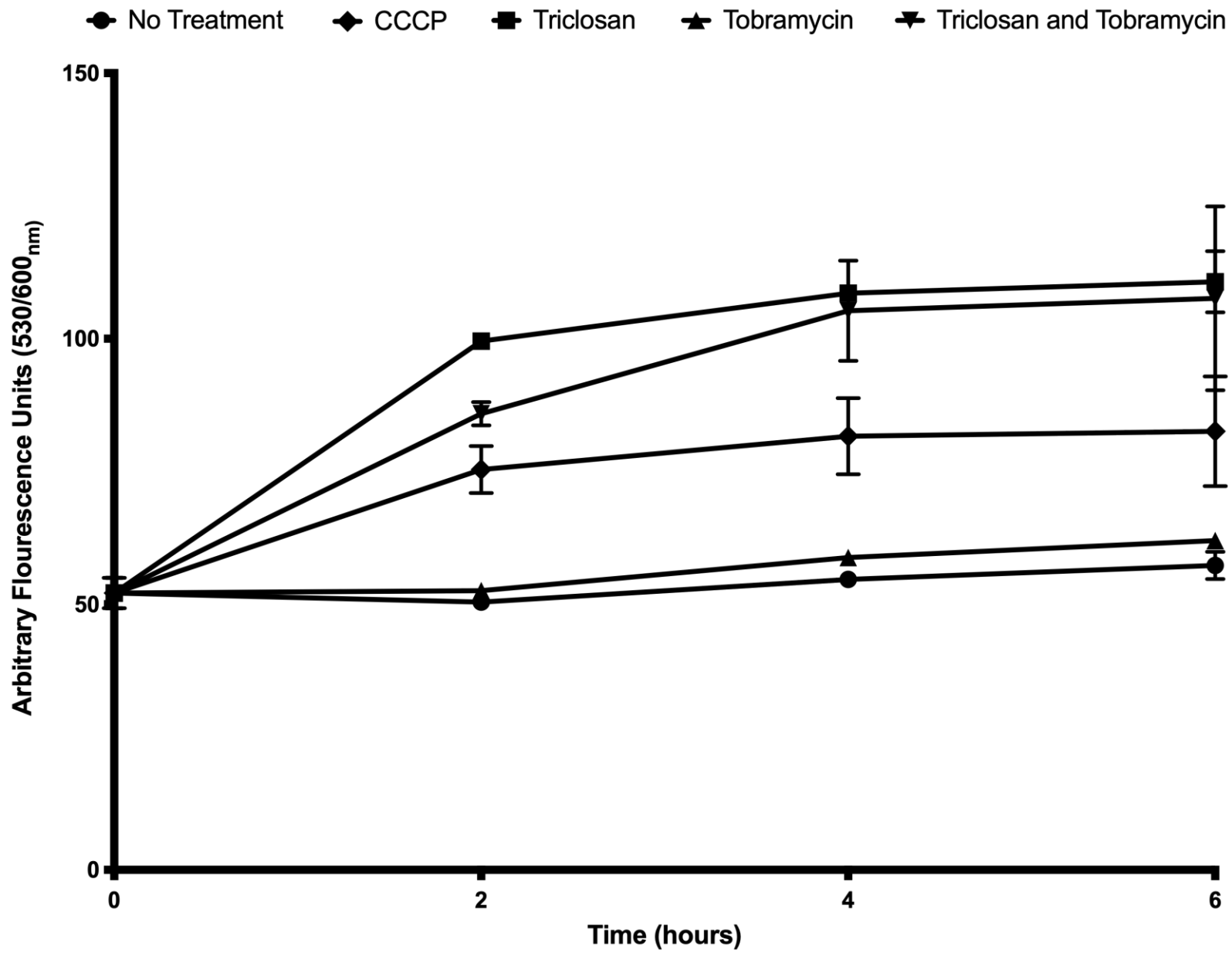

FIG 3. Triclosan reduces the activity of RND-type efflux pumps. 24-hr biofilms were stained with ethidium bromide to measure accumulation. Biofilms were treated with CCCP (100 µM), triclosan (100 µM), tobramycin (500 µM) alone and in combination. Fluorescence was read at 0,2,4, and 6-hrs. Results represent the average arbitrary fluorescence units ±SEM (n=6).

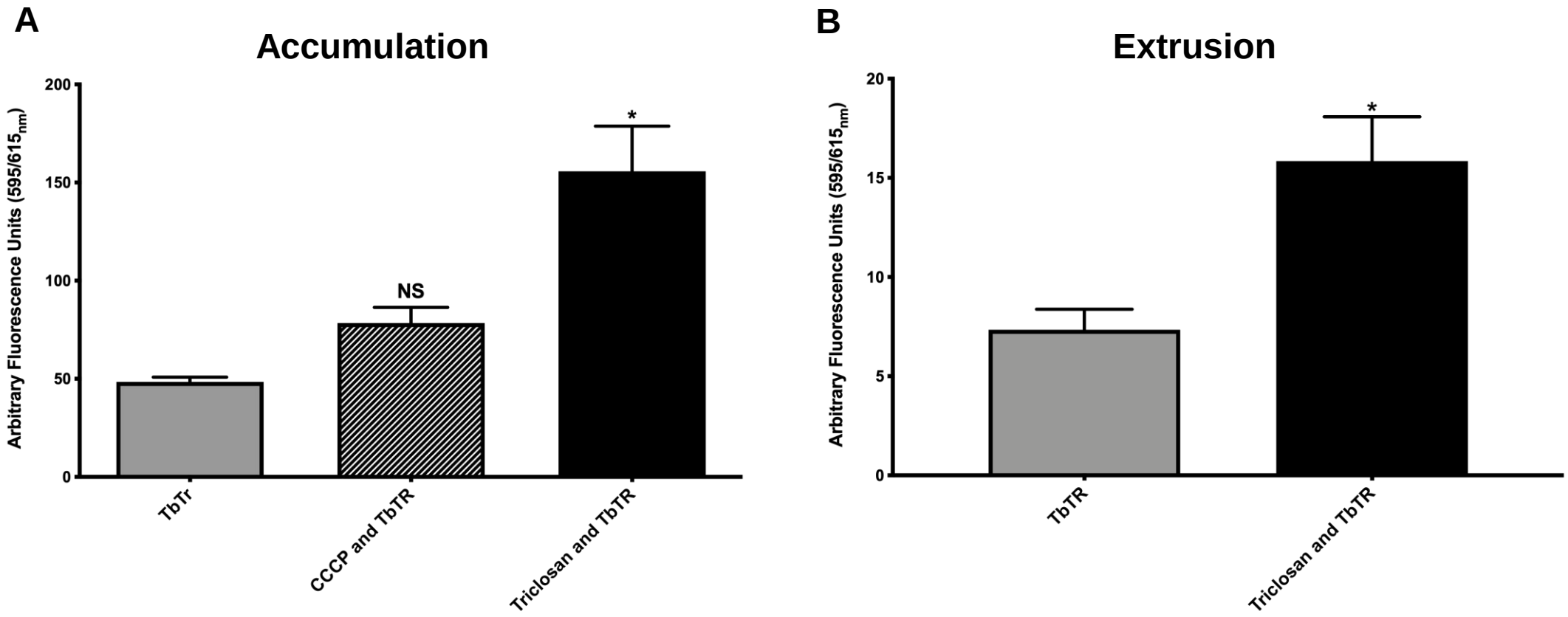

FIG 4. Triclosan results in increased cellular accumulation and extrusion of Texas Red conjugated tobramycin (TbTR). 24-hr old biofilms grown in glass test tubes were treated for 30-mins with triclosan (100 µM), CCCP (100 µM) and TbTR (250 µg/mL). (A) Then cells were disrupted from the biofilms and lysed with 0.2% Triton-X 100® to measure intercellular accumulation of TbTR. (B) To measure extrusion, biofilms were first treated for 30-mins and washed three-times in DPBS. Biofilms then recovered in treatment free media for 30-mins and fluorescence of the media was measured. TbTR was measured by relative fluorescence units using excitation 595_{nm} and emission 615_{nm}. Results represent the average arbitrary fluorescence units ±SEM (n=6). For panel A, a One-Way-ANOVA was performed comparing TbTR alone vs CCCP and TbTR and vs triclosan and TbTR. For panel B, an unpaired t-test was performed comparing TbTR versus triclosan and TbTR. *, $p<0.05$. NS, not significant.

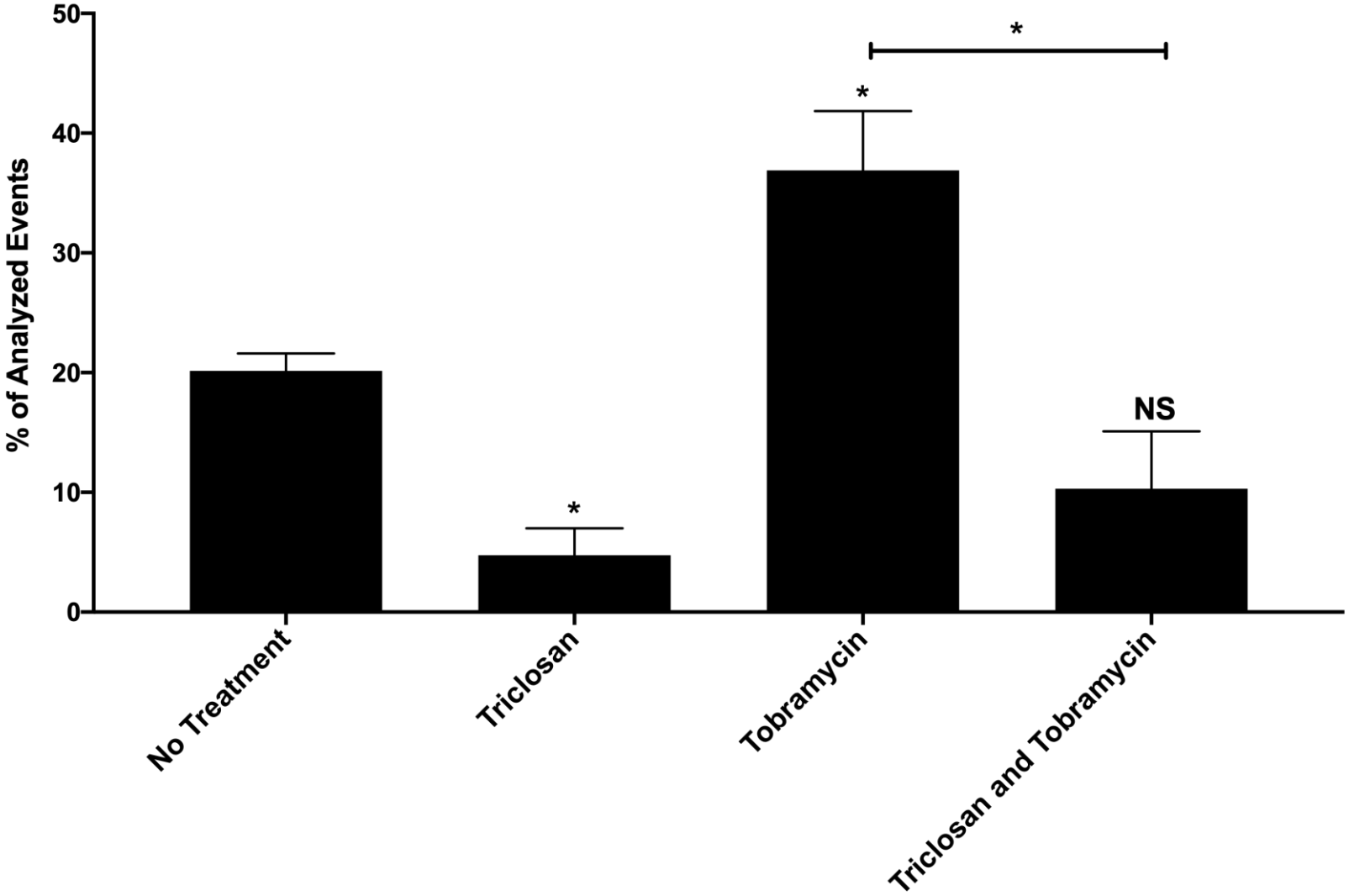

FIG 5. Triclosan reduces the membrane potential surge induced by tobramycin at 2-hours. 24-hr old biofilms were treated with triclosan (100 µM), or tobramycin (500 µM), alone and in combination for 2-hrs. Cells were stained with DiOC2(3) to measure the membrane potential. Dead or permeabilized cells were excluded from membrane potential analysis by parallel staining with the dead cell indicator TO-PRO™-3 iodide. The results are percent averages plus the SEM (n=4). Percent values indicate the average relative abundance of events within each gate normalized to the total number of events analyzed, excluding dead cells, artifacts, aggregates and debris. A one-way ANOVA followed by Sidak's multiple comparison post-hoc test was used to determine statistical significance between each treatment and the untreated control, and tobramycin treatment alone was compared with the combination. *, $p<0.05$. NS, not significant.

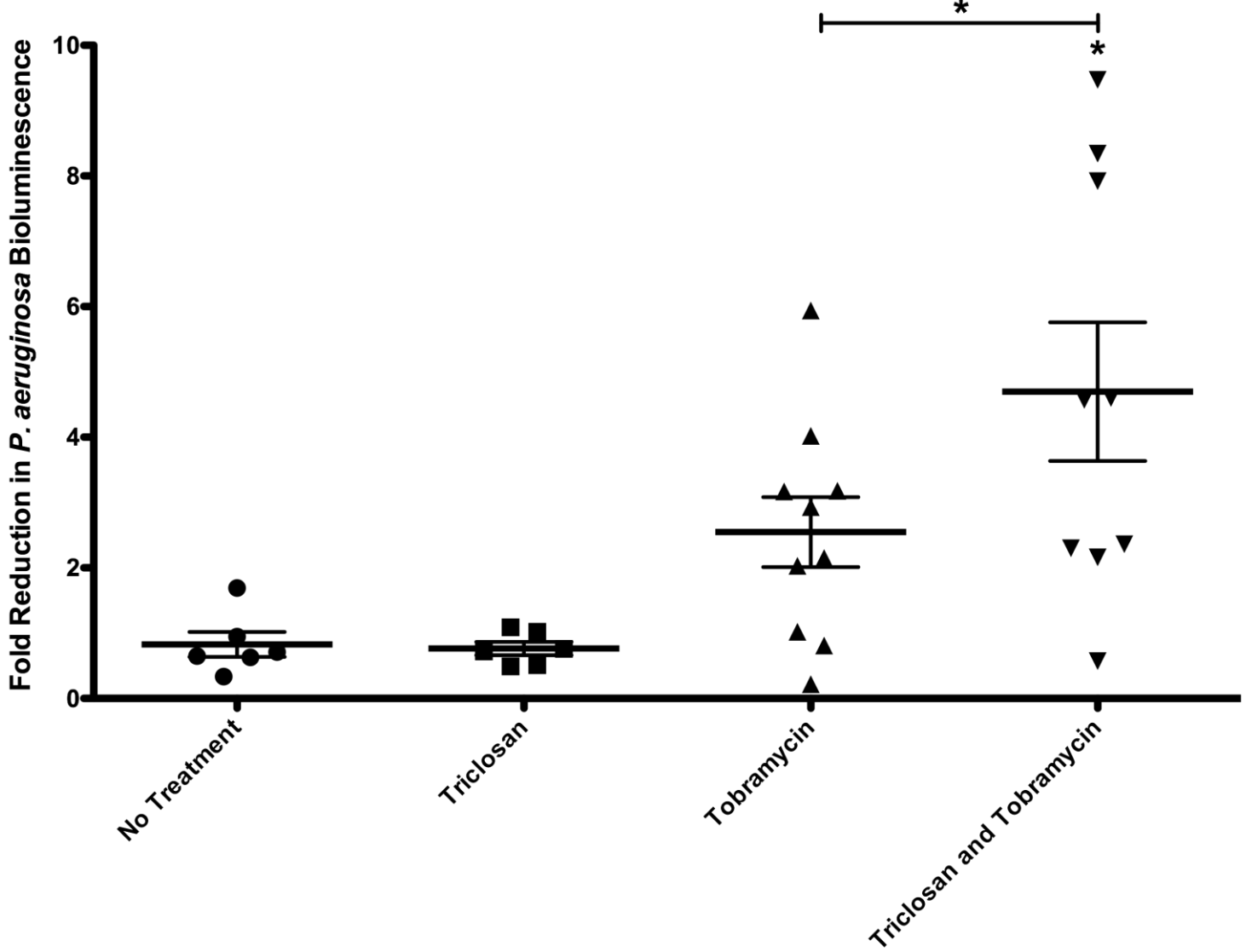

FIG 6. Triclosan and tobramycin hydrogels are more effective than tobramycin hydrogels in a murine wound model. 24-hr old bioluminescent biofilms formed within wounds were treated with triclosan (100 µM), or tobramycin (400 µM), alone and in combination for 4-hrs in a hydrogel. Reduction in the number of cells within biofilms was quantified using IVIS. The results are fold reduction of three separate experiments ±SEM, no treatment n=6, triclosan n=6, tobramycin n=10, triclosan and tobramycin n=9. A one-way ANOVA followed by Bonferroni's multiple comparison post-hoc test was used to determine statistical significance between each treatment and the untreated control and tobramycin treatment alone was compared with tobramycin and triclosan (*, $p<0.05$).

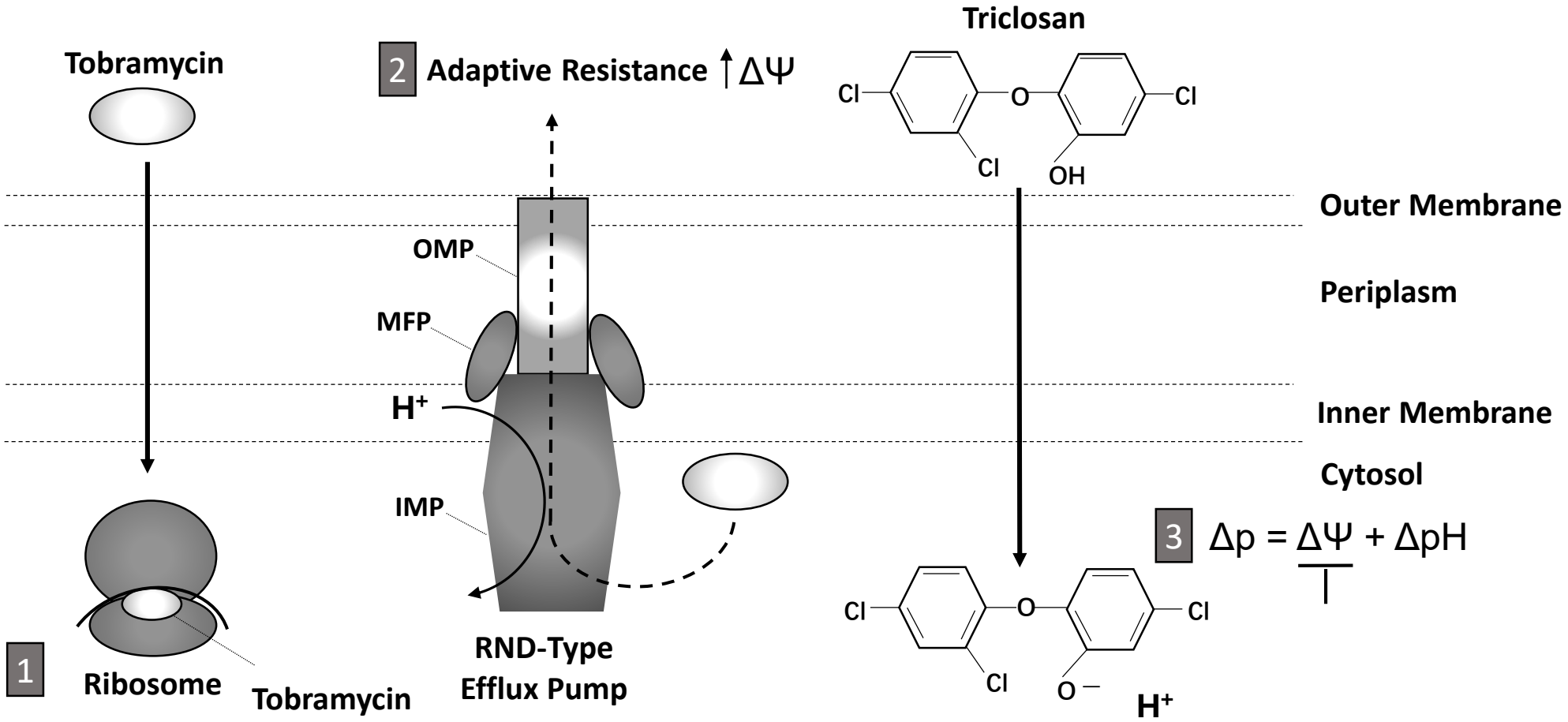

FIG 7. Triclosan sensitizes *P. aeruginosa* to tobramycin by acting as a protonophore, inhibiting efflux pump activity, and abolishing adaptive resistance. (1) Within 2-hrs of exposure to tobramycin, adaptive resistance occurs, (2) which is due to the induction of RND-type efflux pumps and surge in membrane potential (Δψ), resulting in reduced accumulation of tobramycin within the cytosol. (3) Triclosan shuttles protons across the inner membrane, collapsing the proton motive force (Δp) and depolarizing the Δψ. Consequently, efflux pump activity is reduced and there is enhanced accumulation of tobramycin within the cytosol. Finally, tobramycin binds to the A-site of the ribosome, corrupting protein synthesis and causing membrane permeabilization. Overall, triclosan accelerates and increase the effectiveness of tobramycin by reducing the Δψ and efflux pump activity. Proton gradient, ΔpH. Outer membrane protein (OMP), membrane fusion protein (MFP), inner membrane protein (IMP).

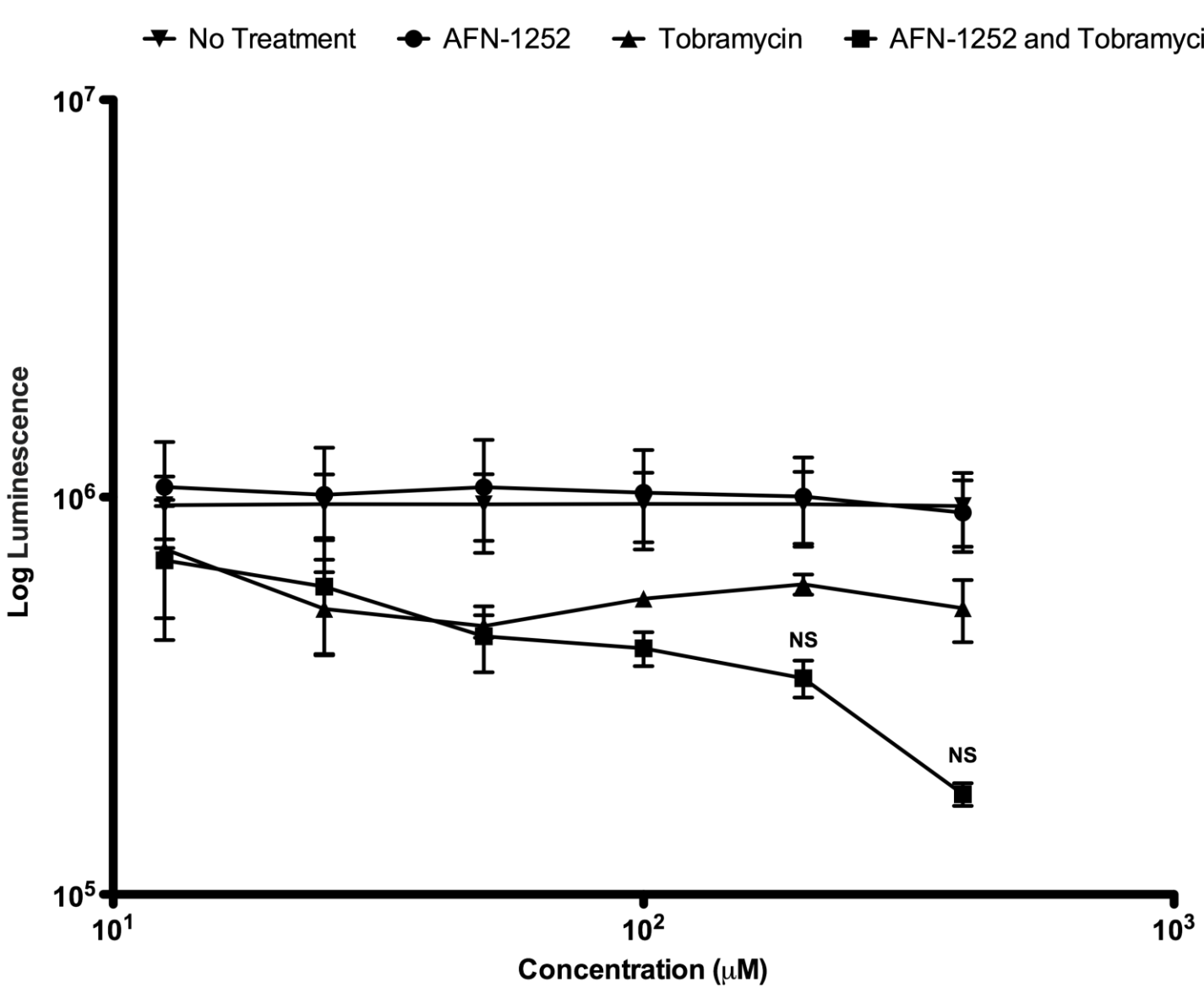

FIG S1. AFN-1252 alone or in combination with tobramycin is not effective against mature biofilms. 24-hr old biofilms grown on MBEC plates were treated for 6-hrs with AFN-1252 (400 µM), tobramycin (400 µM), alone and in combination in two-fold dilutions, and the number of viable cells within the biofilms were quantified by BacTiter-Glo™. The assay was performed twice in in duplicate. The results represent means ± the Standard Error Mean (SEM). A one-way analysis of variance (ANOVA) followed by Bonferroni's multiple comparison post-hoc test was used to determine statistical significance between tobramycin versus the combination (NS, not significant).

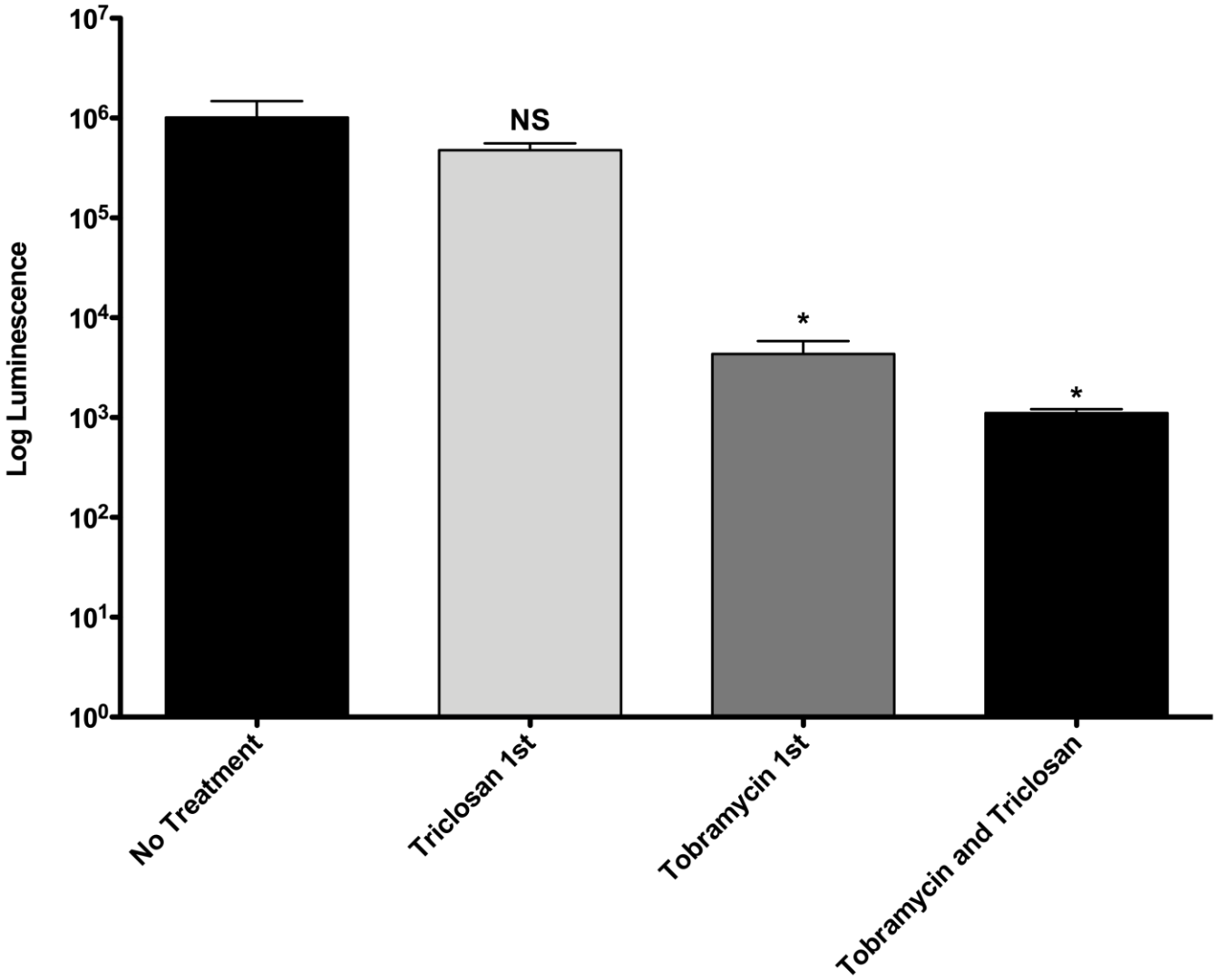

FIG S2. Initial tobramycin treatment is required for the combination to be effective. 24-hr old biofilms grown on MBEC plates were treated sequentially. First, biofilms were treated for 3-hours with tobramycin (500 µM) and then washed three times in DPBS for 3-mins each, before being treated with triclosan (100 µM) for 3-hours or vice versa. As a control, biofilms were also treated for 6-hrs with triclosan and tobramycin. The number of viable cells within the biofilms were quantified by BacTiter-Glo™. The assay was performed twice in in duplicate. The results represent means plus the SEM. A one-way ANOVA followed by Bonferroni's multiple comparison post-hoc test was used to determine statistical significance between each treatment and the untreated control. *, $p<0.05$. NS, not significant.

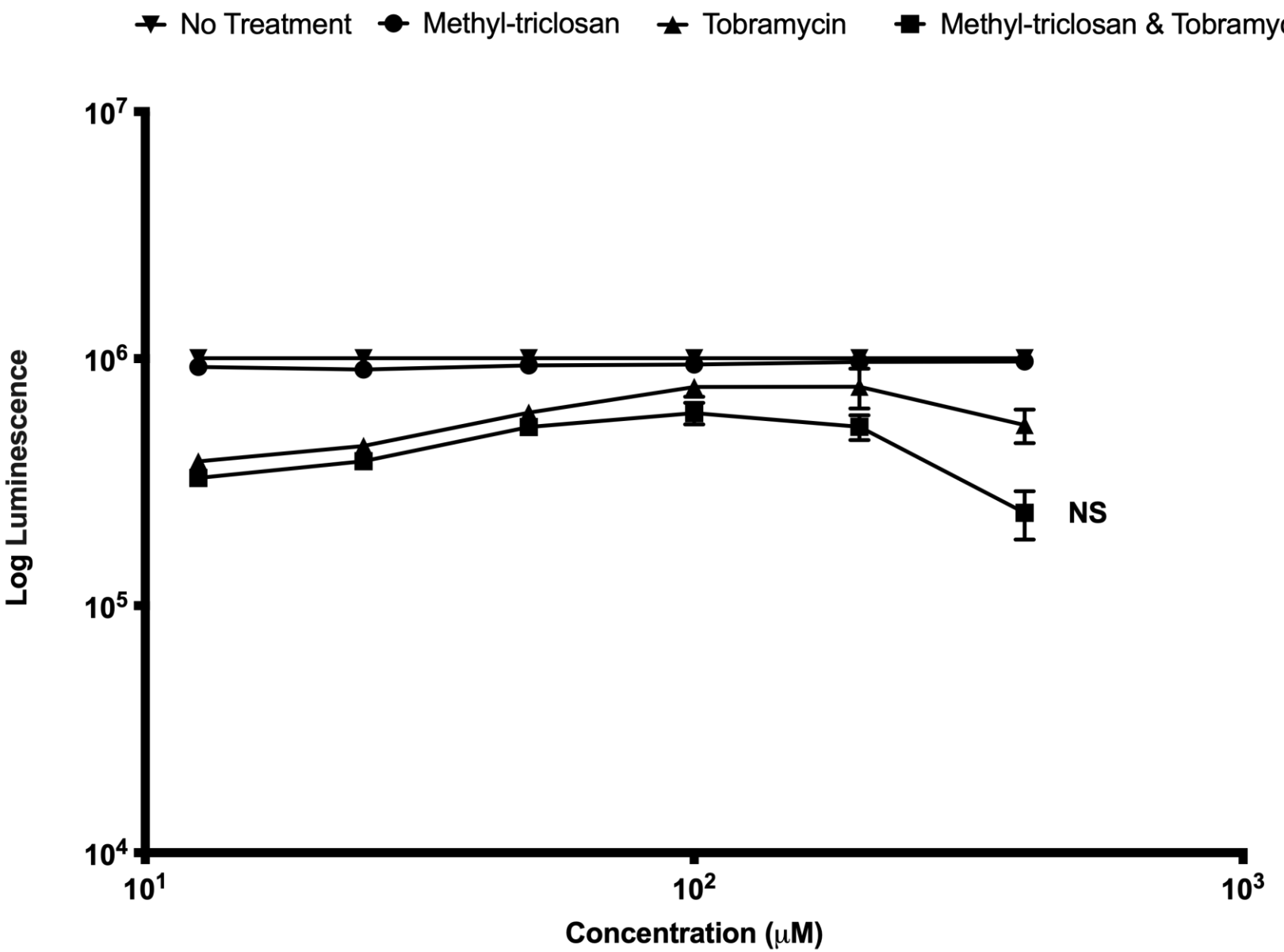

FIG S3. Methyl-triclosan alone or in combination with tobramycin is not effective against mature biofilms. 24-hr old biofilms grown on MBEC plates were treated for 6-hrs with methyl-triclosan (100 µM), tobramycin (400 µM), alone and in combination in two-fold dilutions, and the number of viable cells within the biofilms were quantified by BacTiter-Glo™. The assay was performed twice in in duplicate. The results represent means ±SEM. A one-way ANOVA followed by Bonferroni's multiple comparison post-hoc test was used to determine statistical significance compared to tobramycin alone and the combination. NS, not significant.

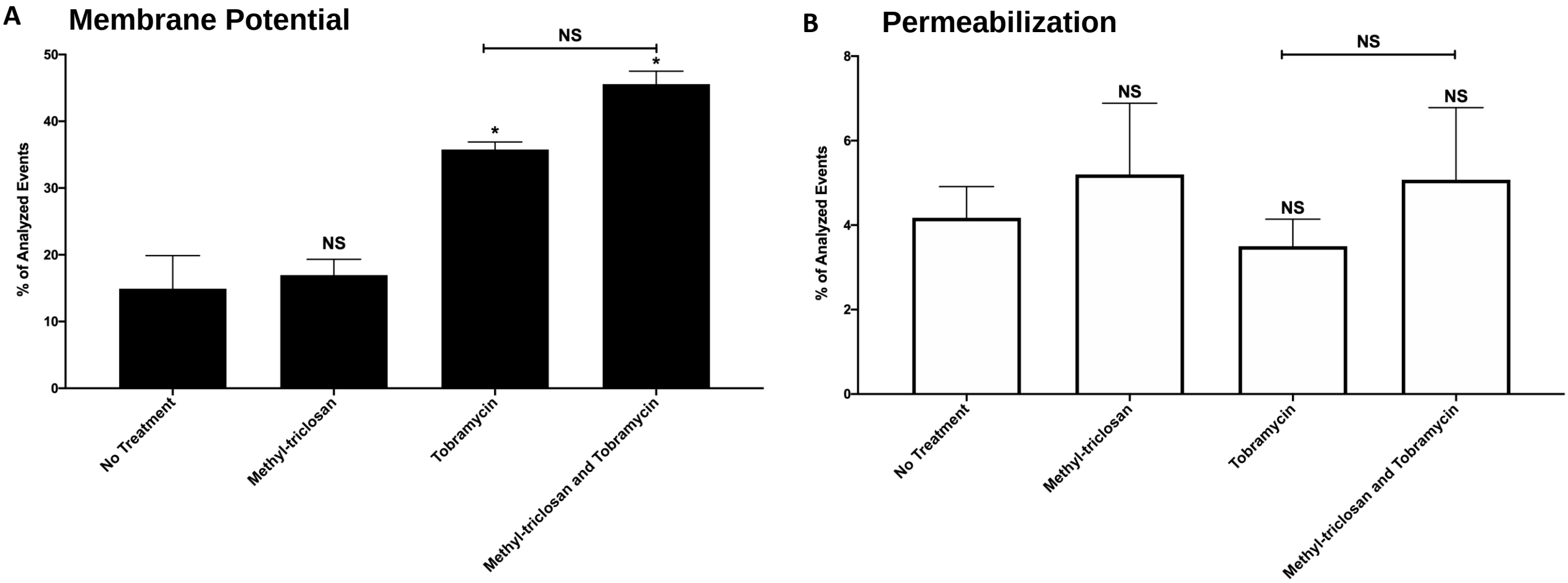

FIG S4. Methyl-triclosan alone and in combination with tobramycin does not reduced the surge in membrane potential induced by tobramycin at 2-hours. 24-hr old biofilms were treated with methyl-triclosan (100 µM), or tobramycin (500 µM), alone and in combination for 2-hrs. Cells were stained with DiOC2(3) and TO-PRO™-3 iodide to determine the number of cells that maintained a membrane potential (A) or were permeabilized (B), respectively. Dead or permeabilized cells were excluded from membrane potential analysis and are shown in panel B. The experiment was performed two separate times in duplicate. The results are percent averages plus the SEM. Percent values indicate the average relative abundance of events within each gate normalized to the total number of events analyzed, excluding artifacts, aggregates and debris. A one-way ANOVA followed by Sidak's multiple comparison post-hoc test was used to determine statistical significance between each treatment and an untreated control, and tobramycin treatment alone was compared with the combination. *, $p<0.05$, NS, not significant.

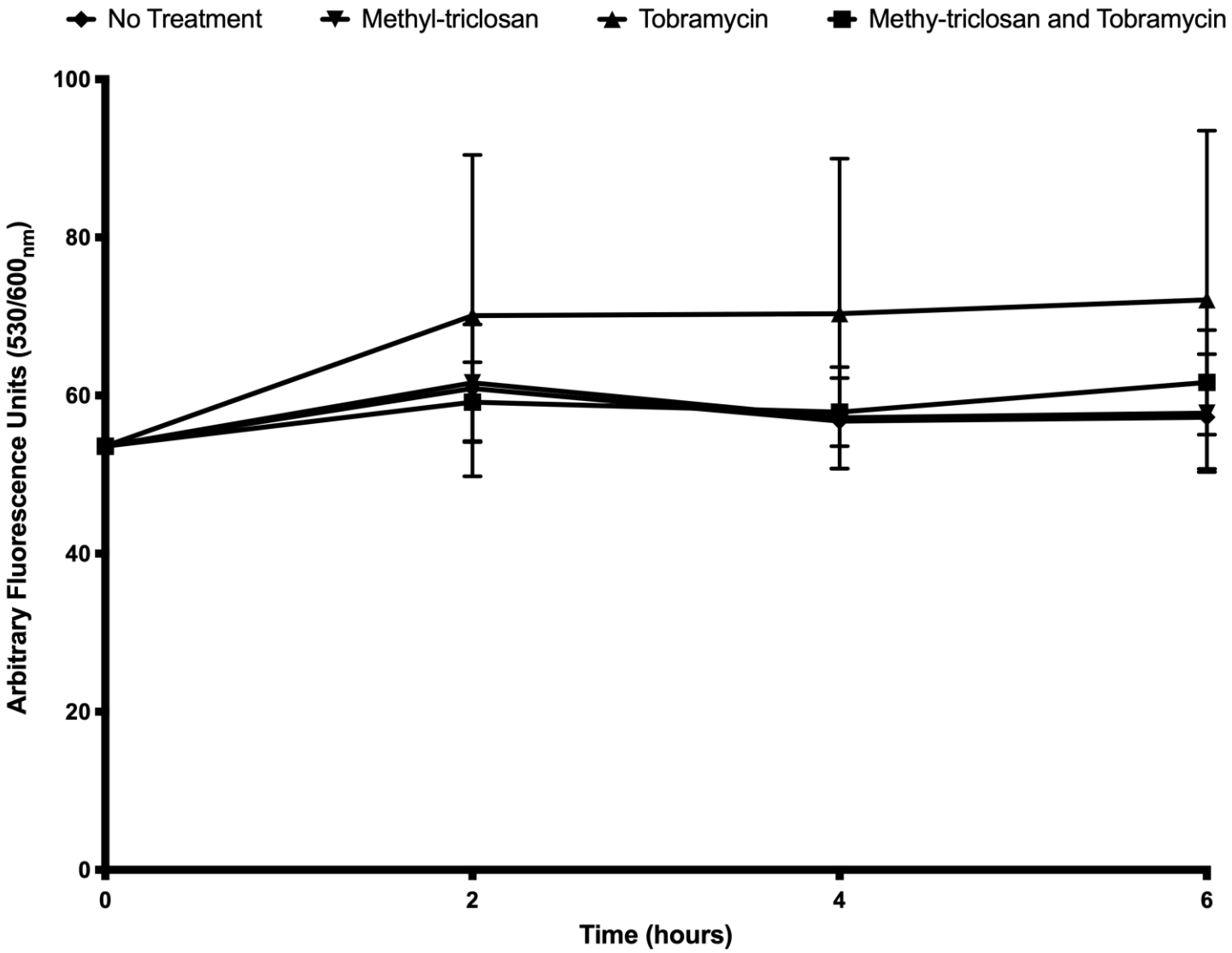

FIG S5. Methyl-triclosan does not reduced RND-type efflux pump activity. Ethidium bromide is a substrate of RND-type efflux pumps. 24-hr biofilms were stained with ethidium bromide to measure accumulation. Biofilms were treated with methyl-triclosan (100 µM) and tobramycin (500 µM) alone and in combination. Fluorescence was read at 0,2,4, and 6-hrs. The assay was performed three times in triplicate. Results represent the average arbitrary fluorescence units ±SEM.

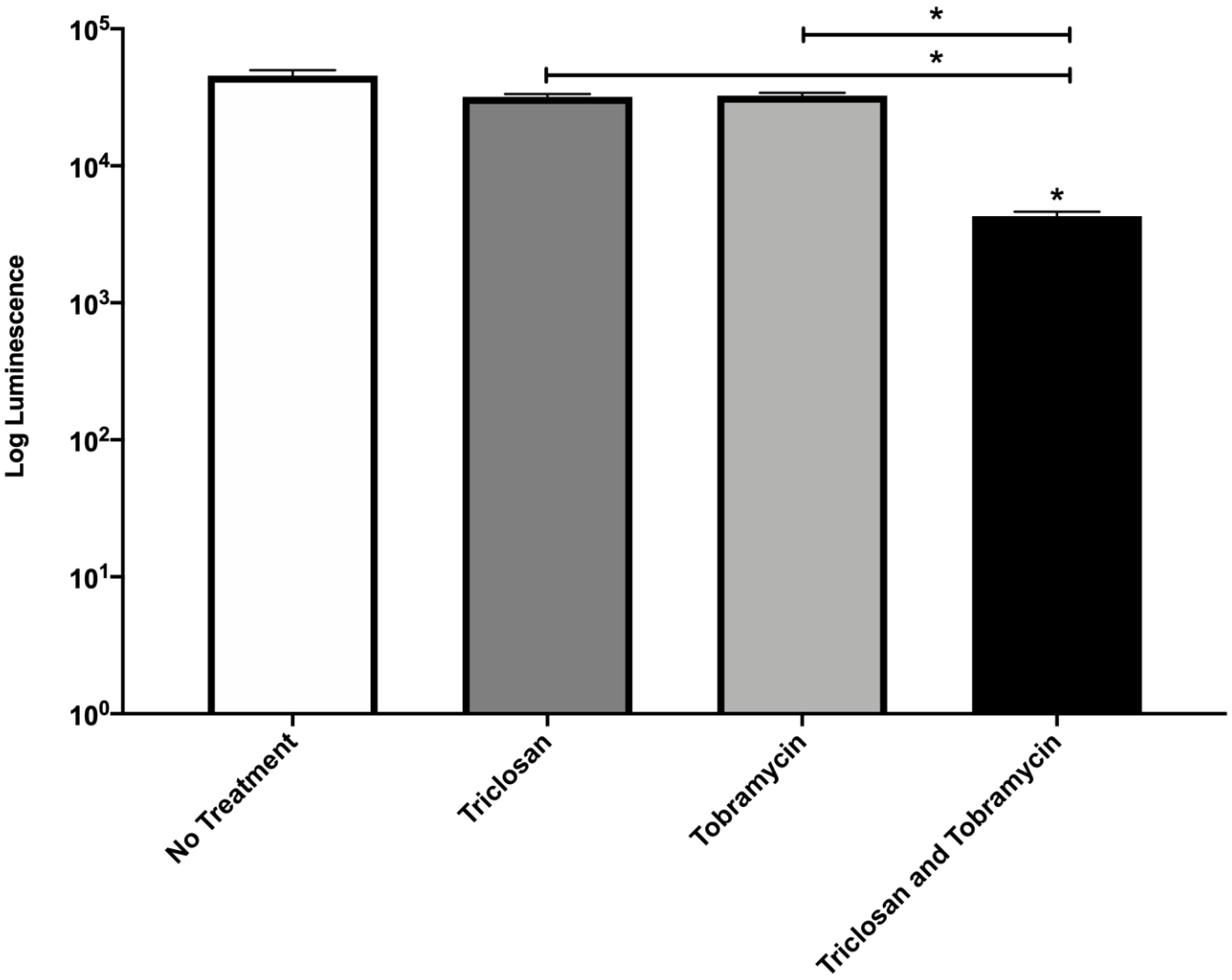

FIG S6. DPBS starved biofilms are not more sensitive to tobramycin alone. 24-hour old biofilms were starved of nutrients by replacing media with DPBS for 5-days. Starved biofilms were treated with triclosan (100 µM), or tobramycin (500 µM), alone and in combination for 6-hrs. The number of viable cells within the biofilms was quantified using the BacTiter-Glo™ assay. The assay was performed once using three biological replicates. The results represent the means plus the SEM. A one-way ANOVA followed by Sidak's multiple comparison post hoc test was used to determine statistical significance between the combination treatment and the untreated control and between triclosan alone or tobramycin alone and the combination treatment as indicated by the bars. *, $P < 0.05$.

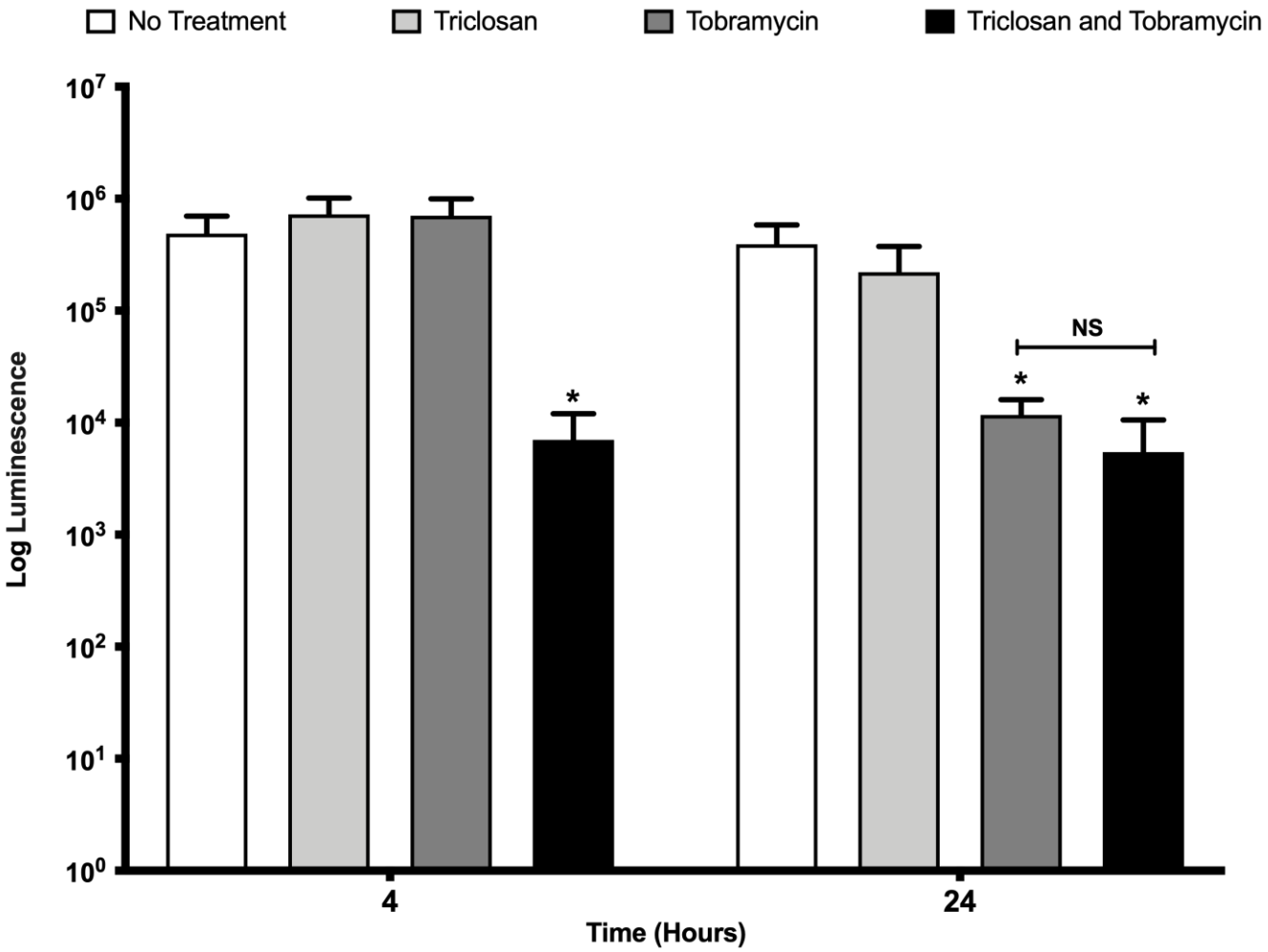

FIG S7. Tobramycin is as effective as the combination after 24-hrs of treatment. 24-hr old biofilms were treated for 24-hrs with triclosan (100 µM), tobramycin (500 µM), alone and in combination, and the number of viable cells within the biofilms were quantified by BacTiter-Glo™. The assay was performed at least three times in triplicate. The results represent means plus the SEM. A one-way ANOVA followed by Bonferroni's multiple comparison post-hoc test was used to determine statistical significance between untreated biofilms, tobramycin alone, and the combination treatment. In addition, using the same analysis, a comparison was made between tobramycin alone and the combination treatment. *, $P < 0.05$. NS, not significant. 4-hr treatments were previously published and are shown for comparison (28).

Table S1. Treatment regimens used for the selection of resistant mutants.

Cycle	Tobramycin	Triclosan	Table Part A
0	0	0	
1	0.00474756	0.47475615	**Gradual Start**
2	0.00678223	0.67822307	
3	0.0096889	0.9688901	
4	0.01384129	1.38412872	
5	0.01977327	1.97732674	
6	0.02824752	2.82475249	
7	0.04035361	4.0353607	
8	0.05764801	5.764801	
9	0.0823543	8.23543	**Moderate Start**
10	0.117649	11.7649	
11	0.16807	16.807	
12	0.2401	24.01	
13	0.343	34.3	
14	0.49	49	
15	0.7	70	
16	1* Tobramycin MIC	100	

Cycle	Tobramycin	Triclosan	Table Part B
17	10	100	**Gradual & Moderate**
18	12.77	110.59	
19	16.30729	122.301481	
20	20.8244093	135.253208	
21	26.5927707	149.576523	
22	33.9589682	165.416676	
23	43.3656024	182.934302	
24	55.3778743	202.307045	
25	70.7175454	223.731361	
26	90.3063055	247.424512	
27	115.321152	273.626768	
28	147.265111	302.603843	
29	188.057547	334.64959	
30	240.149488	370.088981	**End**

27 *P. aeruginosa* biofilms serially passaged in parallel were exposed to sudden, moderate, and gradual treatment regimens consisting of ever-increasing concentrations of tobramycin and triclosan spread out over longer and longer periods of time, as shown in the table above. Gradual and moderate treatment groups were started at different concentrations of tobramycin and triclosan. However, they were then treated in subsequent cycles with ever increasing concentrations of triclosan and tobramycin at the same rate. For example, the moderate treatment group reached 1 μM of tobramycin and 100 μM of triclosan in 8-cycles, whereas the gradual treatment group reached the same concentration in 16-cycles from their initial treatments. The sudden treatment series was treated with 500 μM of triclosan and tobramycin from cycle day 1 and was eradicated, thus, is not shown in the table. MIC, minimum inhibitory concentration.